ORGANOMETALLICS
Article

Organometallics **2010,** *29,* 835–846 835
DOI: 10.1021/om900943m

Coupling of Aromatic N-Heterocycles Mediated by Group 3 Complexes

Colin T. Carver, Bryan N. Williams, Kevin R. Ogilby, and Paula L. Diaconescu*

Department of Chemistry & Biochemistry, University of California, Los Angeles, California 90095

Received October 27, 2009

Group 3 η^2-N,C-pyridyl complexes supported by a ferrocene-diamide ligand have been known to mediate the coupling of η^2-N,C-pyridyl and coordinated-pyridine ligands with a concomitant dearomatization of the pyridine ligand. Examples reported previously by us were limited to a few cases. In order to investigate the scope of the coupling reaction, various η^2-N,C-pyridyl scandium complexes were isolated and characterized. Their reactivity toward other aromatic N-heterocycles is presented along with the characterization of the subsequent reaction products. The coupling reaction is favored by *ortho* substitution, the presence of fused aromatic rings on the pyridine ligand, and chelating substrates. In one instance, the product of the coupling reaction between a scandium η^2-N,C-pyridyl complex and 7,8-benzoquinoline could not be isolated because a subsequent isomerization reaction was favored. The coupling reaction is not restricted to η^2-N,C-pyridyl fragments, and it proceeds also from CH_2 groups bound to the metal center and connected to a pyridine ligand. The reaction between η^2-N,C-imidazolyl scandium complexes and 2,2′-bipyridine is also discussed.

Introduction

Alkyl complexes of d^0f^n metal centers have been shown to react with C−H bonds by σ-bond metathesis.[1−3] Among substrates for C−H activation, aromatic N-heterocycles represent an important class of compounds because of their relevance to biology[4−7] and to the hydrodenitrogenation (HDN) process.[8−14] In some cases, the C−H activation event is coupled with functionalization reactions, such as the insertion of unsaturated substrates, leading to derivative heterocyclic structures.[15−24]

We have reported that d^0f^n benzyl complexes[25,26] supported by a ferrocene-diamide ligand, NN^{fc} (NN^{fc} = fc-$(NSi^tBuMe_2)_2$, fc = 1,1′-ferrocenylene), show diverse reactivity with aromatic N-heterocyclic substrates.[27−30] In all cases studied by us so far, the initial C−H activation event was followed by the coupling of two N-heterocycles, leading to the dearomatization of one of the substrates. We have also observed that this dearomatization poises the heterocycle for ring-opening (1-methylimidazole, Scheme 1)[29,30] or isomerization (pyridines, Scheme 2).[28] Since the coupling reaction is common to both types of subsequent reactivity, we became interested in determining its scope when group 3 alkyl complexes are involved. Previous to our work, examples of metal-mediated coupling of pyridines were limited to

*Corresponding author. E-mail: pld@chem.ucla.edu.

(1) Watson, P. L. *J. Am. Chem. Soc.* **1983**, *105*, 6491–6493.
(2) Thompson, M. E.; Baxter, S. M.; Bulls, A. R.; Burger, B. J.; Nolan, M. C.; Santarsiero, B. D.; Schaefer, W. P.; Bercaw, J. E. *J. Am. Chem. Soc.* **1987**, *109*, 203–219.
(3) Bercaw, J. E. *Pure Appl. Chem.* **1990**, *62*, 1151–1154.
(4) *Comprehensive Heterocyclic Chemistry II*; Katritzky, A. R.; Rees, C. W.; Scriven, E. F. V., Eds.; Pergamon: Oxford, 1996.
(5) *Advances in Heterocyclic Chemistry*; Gilchrist, T. L., Gribble, G. W., Eds.; Pergamon: Oxford, 1999; Vol. *11*.
(6) Joule, J. A.; Mills, K. *Heterocyclic Chemistry*; Blackwell Science: Oxford, 2000.
(7) Katritzky, A. R.; Pozharskii, A. F. *Handbook of Heterocyclic Chemistry*; Pergamon: Oxford, 2003.
(8) Katzer, J. R.; Sivasubramanian, R. *Catal. Rev.-Sci. Eng.* **1979**, *20*, 155–208.
(9) Ho, T. C. *Catal. Rev.-Sci. Eng.* **1988**, *30*, 117–160.
(10) Perot, G. *Catal. Today* **1991**, *10*, 447–472.
(11) Prins, R. In *A Handbook of Heterogeneous Catalysis*; Ertl, G., Knözinger, H., Weitkamp, J., Eds.; VCH Verlagsgesellschaft: Weinheim, Germany, 1997.
(12) Kabe, T.; Ishikawa, A.; Qian, W. *Hydrodesulfurization and Hydrodenitrogenation*; Wiley-VCH: Chichester, UK, 1999.
(13) Furimsky, E.; Massoth, F. E. *Catal. Rev.-Sci. Eng.* **2005**, *47*, 297−489, and references therein.
(14) Diaconescu, P. L. *Curr. Org. Chem.* **2008**, *12*, 1388–1405.
(15) Jordan, R. F.; Taylor, D. F. *J. Am. Chem. Soc.* **1989**, *111*, 778–779.
(16) Jordan, R. F.; Taylor, D. F.; Baenziger, N. C. *Organometallics* **1990**, *9*, 1546–1557.
(17) Jordan, R. F.; Guram, A. S. *Organometallics* **1990**, *9*, 2116–2123.
(18) Guram, A. S.; Jordan, R. F. *Organometallics* **1990**, *9*, 2190–2192.
(19) Guram, A. S.; Jordan, R. F.; Taylor, D. F. *J. Am. Chem. Soc.* **1991**, *113*, 1833–1835.
(20) Guram, A. S.; Jordan, R. F. *Organometallics* **1991**, *10*, 3470–3479.
(21) Sadow, A. D.; Tilley, T. D. *J. Am. Chem. Soc.* **2003**, *125*, 7971–7977.
(22) Fontaine, F. G.; Tilley, T. D. *Organometallics* **2005**, *24*, 4340–4342.
(23) Sadow, A. D.; Tilley, T. D. *J. Am. Chem. Soc.* **2005**, *127*, 643–656.
(24) Barros, N.; Eisenstein, O.; Maron, L.; Tilley, T. D. *Organometallics* **2006**, *25*, 5699–5708.
(25) Carver, C. T.; Monreal, M. J.; Diaconescu, P. L. *Organometallics* **2008**, *27*, 363–370.
(26) Monreal, M. J.; Diaconescu, P. L. *Organometallics* **2008**, *27*, 1702–1706.
(27) Carver, C. T.; Diaconescu, P. L. *J. Alloys Compd.* **2009**, *488*, 518–523.
(28) Carver, C. T.; Benitez, D.; Miller, K. L.; Williams, B. N.; Tkatchouk, E.; Goddard, W. A.; Diaconescu, P. L. *J. Am. Chem. Soc.* **2009**, *131*, 10269–10278.
(29) Carver, C. T.; Diaconescu, P. L. *J. Am. Chem. Soc.* **2008**, *130*, 7558–7559.
(30) Monreal, M. J.; Khan, S.; Diaconescu, P. L. *Angew. Chem., Int. Ed.* **2009**, *48*, 8352–8355.

Published on Web 01/14/2010

Scheme 1. Ring-Opening of 1-Methylimidazole Mediated by the Scandium Alkyl Complex 1-CH_2Ar

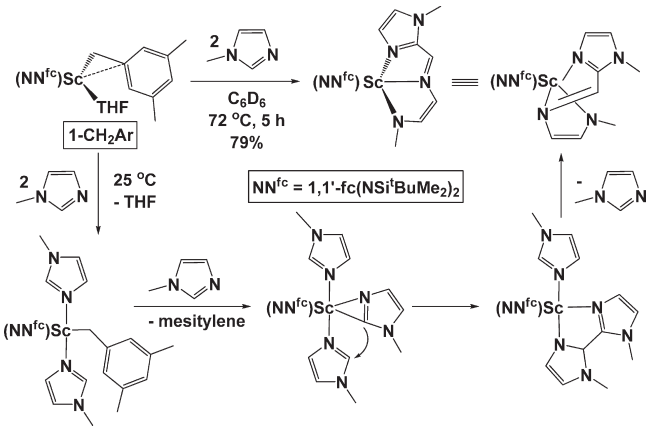

Scheme 2. Coupling of Pyridines and Subsequent Isomerization Mediated by the Scandium Alkyl Complex 1-CH_2Ar

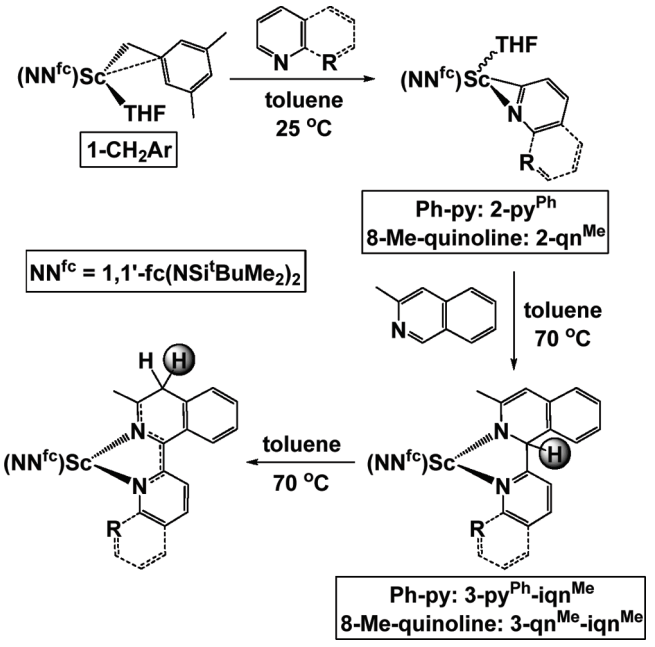

alkali metals,[31] tantalum,[32] and one uncharacterized complex of yttrium.[33]

Results and Discussion

As reported earlier, the reaction between $(NN^{fc})Sc(CH_2Ar)(THF)$ (**1-CH_2Ar**, Ar = 3,5-$Me_2C_6H_3$) and 2-phenylpyridine or 8-methylquinoline led to the corresponding *ortho*-metalated[2,14,17,34−49] complex **2-py^{Ph}** or **2-qn^{Me}**, respectively, as the THF adduct (Scheme 2).[28,29] Although two isomers may exist for **2-py^{Ph}** or **2-qn^{Me}**, depending on the relative orientation of the pyridyl and the coordinated THF ligands, only one isomer was observed in solution for both cases. For 2-phenylpyridine, it is difficult to make a definitive structural assignment, since the isomer containing the THF ligand coordinated next to the η^2-N,C-pyridyl nitrogen atom was more stable by only 0.9 kcal/mol than the one for which THF is coordinated next to the η^2-N,C-pyridyl carbon atom, as assessed from DFT calculations. Furthermore, a different situation was observed for the product of the reaction between $(NN^{fc})Sc(Me)(THF)_2$ and pyridine that forms $(NN^{fc})Sc(\eta^2$-N,C-pyridyl)(py), which was crystallographically characterized and showed that pyridine was coordinated next to the η^2-N,C-pyridyl nitrogen atom.[27] DFT calculations agreed with the experimental findings and indicated that for $(NN^{fc})Sc(\eta^2$-N,C-pyridyl)(py) the isolated compound was more stable by 31.2 kcal/mol than its isomer. However, for 8-methylquinoline, the difference between the two isomers was 11.4 kcal/mol, in favor of the isomer for which the THF ligand was coordinated next to the η^2-N,C-pyridyl carbon atom. The Jordan group has also reported that η^2-N,C-pyridyl zirconocene complexes exist as single isomers in solution, with the exception of quinoline and 7,8-benzoquinoline, when both isomers were observed in solution.[50]

The C−H activation reaction was extended to 2-trimethylsilylpyridine, 2,6-lutidine, 7,8-benzoquinoline, and acridine to give **2-py^{Si}**, **2-lut**, **2-bqn**, and **2-acr**, respectively (Scheme 3). All the reactions were carried out in toluene for 16 h, and the reaction temperatures varied from room temperature (**2-bqn**), to 35 °C (**2-py^{Si}**), 50 °C (**2-lut**), and 70 °C (**2-acr**). All the isolated products, except **2-py^{Si}**, were sparingly soluble in hexanes and readily soluble in toluene and showed colors varying from yellow (**2-py^{Si}**, **2-lut**) to orange (**2-acr**) and red (**2-bqn**). The yields of all reactions were very good, ranging from 76% for **2-acr** to 99% for **2-lut**; the new complexes were characterized by elemental analysis and ^1H and ^{13}C NMR spectroscopy. Since only one isomer was observed in solution for **2-py^{Si}**, **2-bqn**, and **2-acr**, DFT calculations and ^1H NMR spectroscopy experiments were used to establish its identity. It was found that for **2-bqn** and **2-acr** the isomer for which THF was coordinated next to the η^2-N,C-pyridyl carbon atom was

(31) Clarke, A. J.; McNamara, S.; Meth-Cohn, O. *Tetrahedron Lett.* **1974**, *15*, 2373–2376.
(32) Soo, H. S.; Diaconescu, P. L.; Cummins, C. C. *Organometallics* **2003**, *23*, 498–503.
(33) Deelman, B.-J.; Stevels, W. M.; Teuben, J. H.; Lakin, M. T.; Spek, A. L. *Organometallics* **1994**, *13*, 3881–3891.
(34) Boaretto, R.; Roussel, P.; Kingsley, A. J.; Munslow, I. J.; Sanders, C. J.; Alcock, N. W.; Scott, P. *Chem. Commun.* **1999**, 1701–1702.
(35) Boaretto, R.; Roussel, P.; Alcock, N. W.; Kingsley, A. J.; Munslow, I. J.; Sanders, C. J.; Scott, P. *J. Organomet. Chem.* **1999**, *591*, 174–184.
(36) den Haan, K. H.; Wielstra, Y.; Teuben, J. H. *Organometallics* **1987**, *6*, 2053–2060.
(37) Dormond, A.; El Bouadili, A. A.; Moïse, C. *J. Chem. Soc., Chem. Commun.* **1985**, 914–916.
(38) Duchateau, R.; Brussee, E. A. C.; Meetsma, A.; Teuben, J. H. *Organometallics* **1997**, *16*, 5506–5516.
(39) Duchateau, R.; van Wee, C. T.; Teuben, J. H. *Organometallics* **1996**, *15*, 2291–2302.
(40) Jantunen, K. C.; Scott, B. L.; Kiplinger, J. L. *J. Alloys Compd.* **2007**, *444−445*, 363–368.
(41) Kiplinger, J. L.; Scott, B. L.; Schelter, E. J.; Pool Davis Tournear, J. A. *J. Alloys Compd.* **2007**, *444−445*, 477–482.
(42) Klei, B.; Teuben, J. H. *J. Chem. Soc., Chem. Commun.* **1978**, 659–660.
(43) Klei, E.; Teuben, J. H. *J. Organomet. Chem.* **1981**, *214*, 53–64.
(44) Pool, J. A.; Scott, B. L.; Kiplinger, J. L. *J. Alloys Compd.* **2006**, *418*, 178–183.
(45) Radu, N. S.; Buchwald, S. L.; Scott, B.; Burns, C. J. *Organometallics* **1996**, *15*, 3913–3915.
(46) Scollard, J. D.; McConville, D. H.; Vittal, J. J. *Organometallics* **1997**, *16*, 4415–4420.
(47) Watson, P. L. *J. Chem. Soc., Chem. Commun.* **1983**, 276–277.
(48) Jantunen, K. C.; Scott, B. L.; Gordon, J. C.; Kiplinger, J. L. *Organometallics* **2007**, *26*, 2777–2781.
(49) Sugiyama, H.; Aharonian, G.; Gambarotta, S.; Yap, G. P. A.; Budzelaar, P. H. M. *J. Am. Chem. Soc.* **2002**, *124*, 12268–12274.
(50) Jordan, R. F.; Guram, A. S. *Organometallics* **1990**, *9*, 2116–2123.

Scheme 3. C−H Activation of Aromatic N-Heterocycles Mediated by 1-CH_2Ar

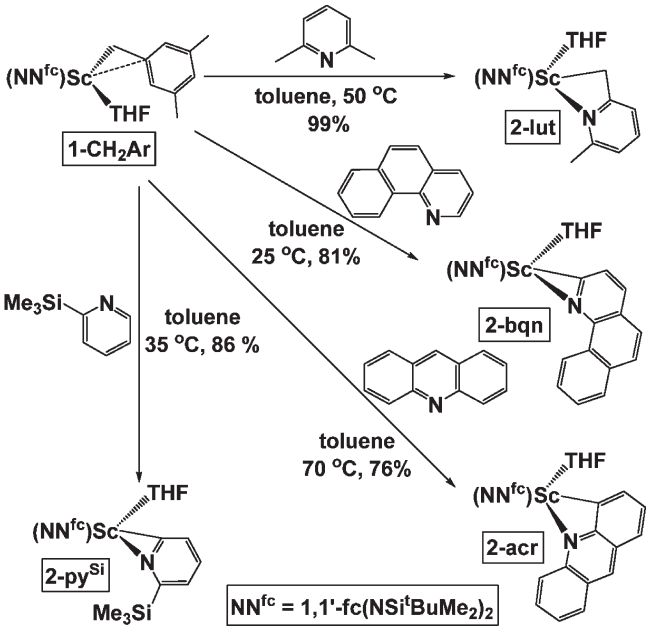

more stable than the one for which THF was coordinated next to the η^2-N,C-pyridyl nitrogen atom (by 9.4 and 34.2 kcal/mol, respectively). For **2-py^{Si}**, DFT calculations on the full molecule indicated that the other isomer was more stable by 2.6 kcal/mol. Given that the calculated energy difference was small, a nuclear Overhauser enhancement spectroscopy (NOESY) experiment was undertaken. The NMR spectroscopy experiment showed that the isomer found in solution was the one corresponding to the drawing in Scheme 3. In order to understand the different results obtained from the DFT calculations and the NOESY experiment, calculations were also carried out by using a solvent correction. When benzene was used as a solvent, the isomer detected by the NOESY experiment was found to be more stable by 2.3 kcal/mol than the other isomer. The new results do not invalidate the calculations for the other complexes since calculations carried out with or without solvent corrections usually follow similar stability trends and such reversals are only to be suspected when one method shows small differences in the energies of the two isomers (likely less than 5 kcal/mol).

The complex **2-lut** was also characterized by X-ray crystallography (Figure 1), which indicated a κ^3-N,C,C-coordination of lutidine: Sc−C_{CH2}, Sc−C_{py}, and Sc−N_{py} distances were 2.3246(20), 2.6804(20) (the sum of the covalent radii for scandium and carbon is 2.46 Å),[51] and 2.2703(16) Å, respectively. The Sc−C_{CH2} distance was slightly longer than that analogous in **1-CH_2Ar** (Sc−C_{CH2Ar}, 2.2640(37) Å),[25] the Sc−C_{py} distance was shorter than the distances between scandium and the *ipso*-carbon atoms of the ferrocene ligand (2.7279(18) and 2.7443(19) Å), and the Sc−N_{py} distance was similar to the distance between scandium and the nitrogen donor of the coordinated pyridine (as opposed to the η^2-N,C-pyridyl one) in (NN^{fc})Sc(η^2-N,C-pyridyl)(py) (2.2758(27) Å).[27]

Next, the reactivity of the newly synthesized pyridyl complexes toward pyridine substrates was investigated.

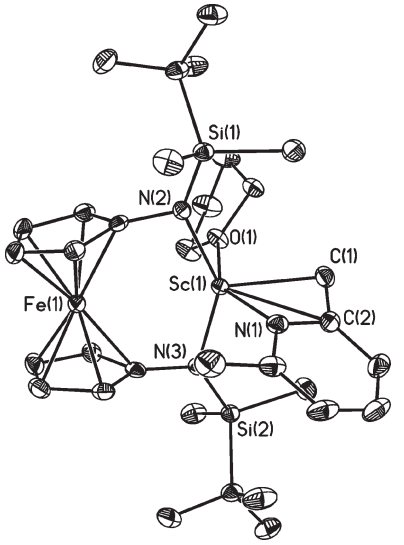

Figure 1. ORTEP representation of **2-lut** with ellipsoids drawn at 50% probability (hydrogen atoms were removed for clarity).

The reaction between **1-CH_2Ar** and excess pyridine gives a mixture of products; by ^{1}H NMR spectroscopy, it was identified that some components of that mixture show signals in the olefinic region of the spectrum. At present, we believe that multiple and competing reaction pathways are possible with pyridine;[28,29] the reaction mixtures proved intractable in our hands. However, as reported earlier,[28,29] if pyridine is replaced by 2-phenylpyridine or 8-methylquinoline, one reaction pathway is favored: the coupling of pyridine rings from the two aromatic heterocycles (Scheme 2, **3-py^{Ph}-iqn^{Me}** and **3-qn^{Me}-iqn^{Me}**). By heating the coupled products **3-py^{Ph}-iqn^{Me}** and **3-qn^{Me}-iqn^{Me}**, a subsequent isomerization took place (Scheme 2).[28] In the course of evaluating substrates that would undergo this isomerization reaction, it was found that the C−C coupling reaction is remarkably general.

The reaction of the complexes **2-py^{Ph}**, **2-py^{Si}**, **2-bqn**, and **2-acr** with various pyridines (phenanthridine, 2,2′-bipyridine, and 3-methylisoquinoline) yielded the products **3-py^{Ph}-phan**, **3-py^{Ph}-bipy**, **3-py^{Si}-iqn^{Me}**, **3-bqn-phan**, and **3-acr-phan**, which ranged in color from blood red to brown (Table 1). During the formation of all these products, the pyridine solvates (the presumed intermediates before the coupling products) could not be isolated or observed by ^{1}H NMR spectroscopy. All the complexes **3** were uniformly less soluble in hydrocarbon solvents than their respective starting materials, a property exploited in the case of **3-py^{Ph}-phan**, **3-bqn-phan**, and **3-acr-phan**, for which analytically pure crystals were collected directly from the reaction mixture by either cooling or addition of *n*-pentane. Complexes **3** are characterized by the chemical shift of the proton on the sp^3 carbon of the dearomatized pyridine that ranges from 8.01 ppm in **3-acr-phan** to 5.84 ppm in **3-py^{Si}-iqn^{Me}**. In agreement with the crystal structures (see below), the coupled products **3** exhibit C_1 symmetry in solution as well, as probed by ^{1}H and ^{13}C spectroscopy (when the collection was practical, see Experimental Section for details), because of the nonplanar arrangement of the two coupled pyridines; the C−H activated complexes **2**, for which the pyridyl and THF ligands could assume a coplanar arrangement, exhibited C_s symmetry in solution.

The complexes **3-py^{Ph}-phan** and **3-acr-phan** were also characterized by X-ray crystallography (Figure 2). Because

(51) Cordero, B.; Gomez, V.; Platero-Prats, A. E.; Reves, M.; Echeverria, J.; Cremades, E.; Barragan, F.; Alvarez, S. *Dalton Trans.* **2008**, 2832–2838.

Table 1. Coupling of Aromatic N-Heterocycles[a]

Compound	Substrate	Product	Product name	Time Yield
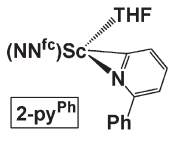	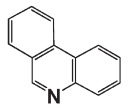	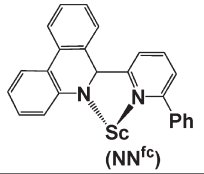	3-py^{Ph}-phan	2 h 77 %
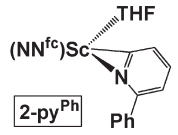	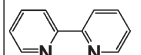	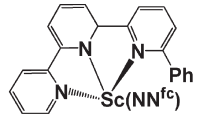	3-py^{Ph}-bipy	16 h 85 %
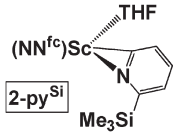	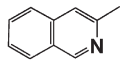	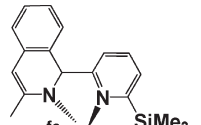	3-py^{Si}-iqn^{Me}	1 h 99 %
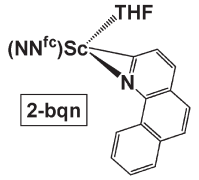	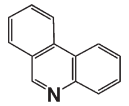	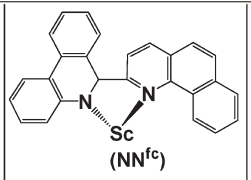	3-bqn-phan	0.5 h 91 %
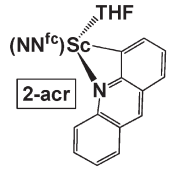	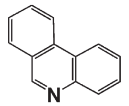	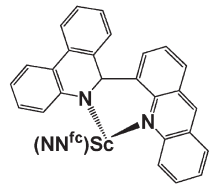	3-acr-phan	16 h 87 %

[a] All reactions occurred in toluene or toluene/*n*-pentane at room temperature.

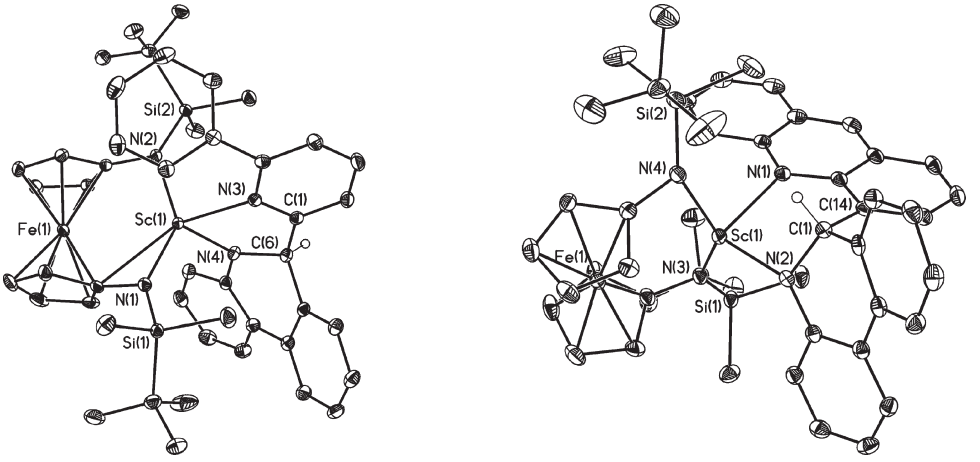

Figure 2. ORTEP representation of **3-py^{Ph}-phan** (left) and **3-acr-phan** (right) with ellipsoids drawn at 50% probability (irrelevant hydrogen atoms were removed for clarity).

of the larger size of the ring formed by coupling in **3-acr-phan** than in **3-py^{Ph}-phan** (six versus five atoms), the two bulky heterocycles in **3-acr-phan** can adopt a perpendicular orientation relative to each other (see Figure SX3b in the Supporting Information for a different view). The increased flexibility of the six-membered ring in **3-acr-phan** also allows the biheterocyclic fragment to come in close proximity to the metal center, as evidenced by the shorter scandium−nitrogen distances in **3-acr-phan** than in **3-py^{Ph}-phan** (Sc−N_{amide}, 2.0690(17) versus 2.0900(12) Å; Sc−N_{py}, 2.2811(17) versus 2.2961(12) Å). Furthermore, the complex **3-acr-phan** features a close contact between scandium and the newly sp^3-hybridized carbon atom (Sc−C distance of 2.8094(20) versus 3.0860(14) Å in **3-py^{Ph}-phan**; the sum of the covalent radii for scandium and carbon is 2.46 Å).[51]

It is also interesting to note that the iron−scandium distance of 3.0063(5) Å in **3-acr-phan** is shorter than that of

Scheme 4. Reaction of 2-py^{Ph} with 7,8-Benzoquinoline

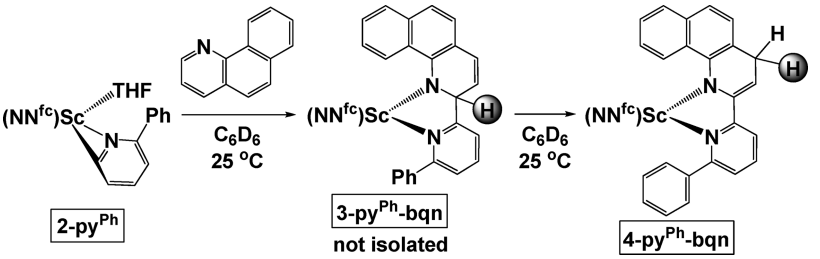

3.1358(4) Å in **3-py^{Ph}-phan**, and it is even shorter than the sum of covalent radii for iron and scandium (3.02 Å).[51] Both these distances are shorter than those in the other two coupled products characterized by X-ray crystallography: 3.2371(11) Å for **3-py^{Ph}-py^{Ph}**[29] and 3.3156(8) Å for **3-py^{Ph}-iqn^{Me}**.[28] It is proposed that this feature is a direct consequence of the steric crowding experienced by the amide substituents of the ferrocene ligand: the more these substituents are likely to interact with the new biheterocyclic fragment, as in **3-acr-phan**, the further apart the two ferrocene nitrogen donors are pushed and the closer the iron center is to scandium. This proposal is supported by the inverse correlation between the scandium−iron and the scandium−N^{fc} distances: the longest Sc−N^{fc} distances are found in **3-acr-phan**: 2.0804(17) and 2.0992(17) Å versus 2.0556(12) and 2.0852(12) Å in **3-py^{Ph}-phan**, 2.0697(36) and 2.0706(35) Å in **3-py^{Ph}-py^{Ph}**, and 2.0505(25) and 2.0665(25) Å in **3-py^{Ph}-iqn^{Me}**.[28]

There are several factors promoting the coupling reactions of the C−H activated complexes **2** with pyridine substrates:

(1) *Ortho*-substituents accelerate the coupling reaction; however, large substituents inhibit it, as evidenced by the fact that in the coupling reaction of **2-py^{Ph}** with 2-phenylpyridine most of **2-py^{Ph}** is recovered and only small amounts of **3-py^{Ph}-py^{Ph}** are formed. These observations are supported by the fact that **3-py^{Ph}-py^{Ph}** was found to be 7.2 kcal/mol higher in energy than the corresponding noncoupled product (see the Supporting Information for details). Although an X-ray crystal structure of **3-py^{Ph}-py^{Ph}** was obtained,[29] the reaction was not facile. In light of the DFT results and experimental observations, it is likely that the formation of **3-py^{Ph}-py^{Ph}** is driven by its decomposition to other stable products (a similar reaction starting from the analogous yttrium complex will be reported elsewhere).

(2) The use of chelating substrates is beneficial, as illustrated by the reaction of **2-py^{Ph}** with 2-phenylpyridine versus that with 2,2′-bipyridine. While the reaction of **2-py^{Ph}** with 2-phenylpyridine was sluggish even at elevated temperatures and the isolation of **3-py^{Ph}-py^{Ph}** in any reasonable yield was difficult, the reaction of **2-py^{Ph}** with 2,2′-bipyridine was facile and the isolation of **3-py^{Ph}-bipy** in high yield was possible (Table 1).

(3) Fused aromatic rings on the coupling partner have an accelerating effect. The reaction of **2-py^{Ph}** with isoquinoline to form **3-py^{Ph}-iqn** was significantly faster than the reaction of **2-py^{Ph}** with 5,6,7,8-tetrahydroisoquinoline, from which no coupling product could be isolated.

The coupling reaction between **2-py^{Ph}** and 7,8-benzoquinoline was also attempted. The monitoring of the reaction mixture by ^{1}H NMR spectroscopy indicated that the conversion to a C_1-symmetric complex, identified as the coupled product **3-py^{Ph}-bqn**, was very slow (several days at room temperature). However, before the formation of **3-py^{Ph}-bqn** was complete, the formation of a second, C_s-symmetric

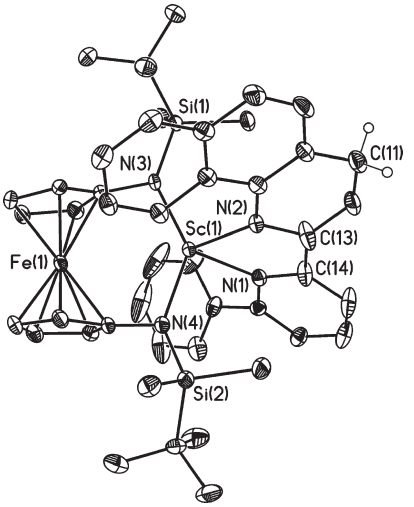

Figure 3. ORTEP representation of **4-py^{Ph}-bqn** with ellipsoids drawn at 50% probability (irrelevant hydrogen atoms were removed for clarity).

product was observed (Scheme 4). The final product was identified as **4-py^{Ph}-bqn**, in which the sp^3-hydrogen atom migrated to the benzyl carbon of the dearomatized pyridine ring (Figure 3).[28] The energy difference between **3-py^{Ph}-bqn** and **4-py^{Ph}-bqn** was calculated to be 6.2 kcal/mol in favor of **4-py^{Ph}-bqn**. It is likely that the activation energy to form **4-py^{Ph}-bqn** is slightly lower than that to form **3-py^{Ph}-bqn**, making the two reactions competitive. Attempts to isolate **3-py^{Ph}-bqn** have been unsuccessful so far.

The complex **4-py^{Ph}-bqn** was characterized by ^{1}H and ^{13}C NMR spectroscopy, X-ray diffraction (Figure 3), and elemental analysis. It is important to note that in order to form **4-py^{Ph}-bqn**, a 1,3-hydrogen migration is required (Scheme 4), an event different than the isomerization reactions previously reported by our group, when a 1,4-hydrogen migration was observed.[28] It is likely that the 1,4-hydrogen migration in **3-py^{Ph}-bqn** is not favorable since it would result in the formation of an sp^3 carbon that would disrupt the aromaticity of the two benzoquinoline phenyl rings, a situation not encountered for the 1,3-hydrogen migration.

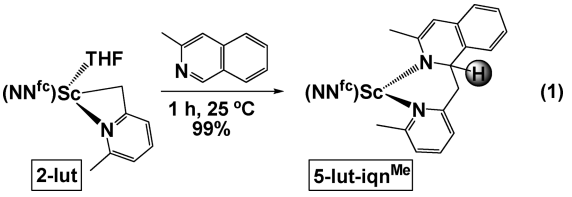

It became apparent that the coupling reaction was not restricted to η^2-N,C-pyridyl complexes when an analogous

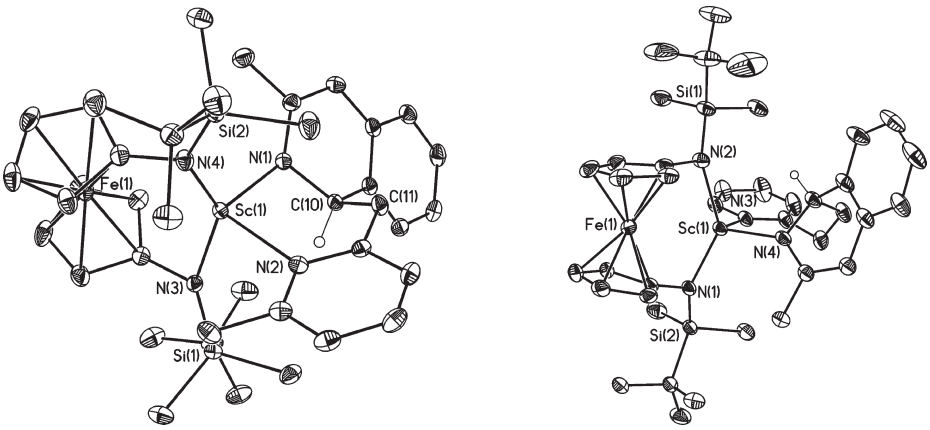

Figure 4. ORTEP representation of **5-lut-iqn^{Me}** (left) and **6-py^{Et}-iqn^{Me}** (right) with ellipsoids drawn at 50% probability (irrelevant hydrogen atoms were removed for clarity).

Scheme 5. Coupling of 2-Picoline and 3-Methylisoquinoline Mediated by 1^{M}-CH$_2$Ph (M = Y, La)

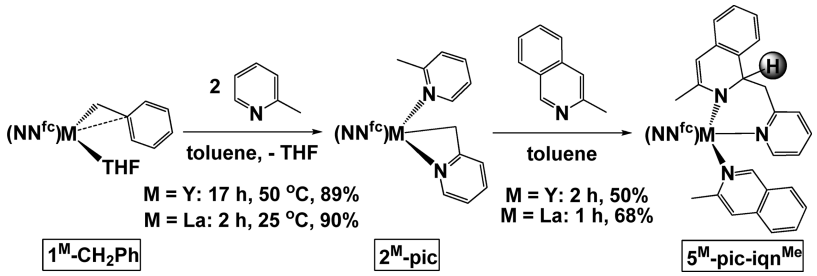

reaction was observed from the CH_2 group of **2-lut** (eq 1). The reaction of **2-lut** with 3-methylisoquinoline led to a coupled product, **5-lut-iqn^{Me}**, in which the two heterocyclic rings were bridged by a methylene group, isolated in 99% yield. The reaction was rather facile; the monitoring of the reaction mixture in C_6D_6 by ^{1}H NMR spectroscopy indicated that the reaction was complete by the time a spectrum could be collected at room temperature. The complex **5-lut-iqn^{Me}** was also characterized by X-ray crystallography (Figure 4). The presence of a methylene group in the six-membered metallocycle allows a near-perpendicular orientation of the two heterocyclic rings, as was observed for **3-acr-phan** (Figure 2).

In order to probe whether the formation of **5-lut-iqn^{Me}** was restricted to scandium complexes, the yttrium and lanthanum compounds obtained by the C−H activation of 2-picoline, **2^{M}-pic** (M = Y, La), were isolated and characterized (Scheme 5). It is interesting to note that the C−H activation of 2-picoline by **1^{M}-CH$_2$Ph** gives exclusively **2^{M}-pic**, featuring an sp^3-C$_{Me}$−M bond instead of an sp^2-C$_{pyridyl}$−M bond. Similar results have been reported for some yttrium[52] and thorium alkyl complexes.[4l] The C−H activation of the methyl group was confirmed by X-ray crystallography for **2^{Y}-pic**. However, because of the poor quality of the data set, it was not possible to determine the exact isomer formed as a consequence of 2-picoline coordination: the one with the methyl group pointing toward the methylene carbon (**2^{Y}-pic**) or the one with the methyl group pointing away from it (**2^{Y}-pic′**). DFT calculations indicated that **2^{Y}-pic** was more stable than **2^{Y}-pic′** by 1.6 kcal/mol, a value that may explain why the two isomers cocrystallized. However, **2^{Y}-pic** is found in solution, as assessed by a ^{1}H NOESY experiment (see the Supporting Information for details). In the case of lanthanum, an analogous experiment showed that the rotation of the coordinated picoline is faster than the NMR spectroscopy time scale at room temperature; at −50 °C, both isomers are present in solution (see the Supporting Information for details). Also, the preferential sp^3 C−H activation is supported by the fact that the four η^2-N,C-pyridyl isomers were all less stable than **2^{Y}-pic** by as little as 5.7 kcal/mol and as much as 13.6 kcal/mol (see the Supporting Information for more details).

The coupling reaction between **2^{M}-pic** and 3-methylisoquinoline (Scheme 4) led indeed to a product, **5^{M}-pic-iqn^{Me}** (M = Y, La), analogous to **5-lut-iqn^{Me}**. One dissimilarity was observed between the complexes of type **5** and the coupled products discussed earlier, **3**: whereas all compounds **3** show markedly different (and more vibrant) colors than their parent compounds **2**, **5-lut-iqn^{Me}** and **5^{M}-pic-iqn^{Me}** are either yellow or orange. The different color change for the two types of coupled products correlates with a larger HOMO−LUMO gap for **5-lut-iqn^{Me}** (0.0455 eV) than for **3-py^{Ph}-iqn^{Me}** (0.0371 eV), as estimated from DFT calculations. Another difference between the complexes **3** and **5** was the fact that, in contrast to **3-py^{Ph}-iqn^{Me}** and **3-qn^{Me}-iqn^{Me}**,[28] prolonged heating of **5-lut-iqn^{Me}** or **5^{M}-pic-iqn^{Me}** did not induce an isomerization reaction (as assessed by ^{1}H NMR spectroscopy).

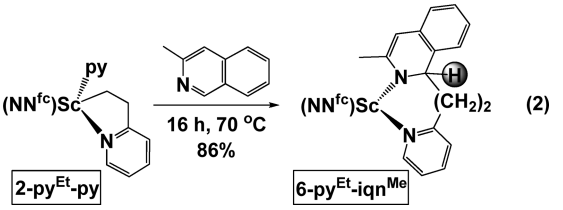

(2)

In light of the somewhat unexpected coupling reactivity of **2-lut** toward 3-methylisoquinoline, the reactivity of the

(52) Duchateau, R.; Brussee, E. A. C.; Meetsma, A.; Teuben, J. H. *Organometallics* **1997**, *16*, 5506–5516.

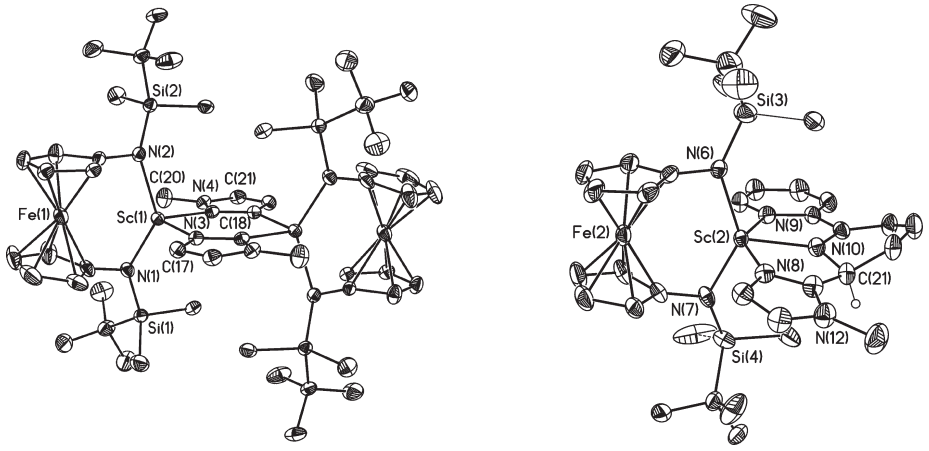

Figure 5. ORTEP representation of $[\mathbf{2\text{-}im}]_2$ (left, thermal ellipsoids drawn at 50% probability) and **3-im-bipy** (right, thermal ellipsoids drawn at 35% probability). Irrelevant hydrogen atoms were removed for clarity.

Scheme 6. Coupling of 1-Methylimidazole and 2,2′-Bipyridine

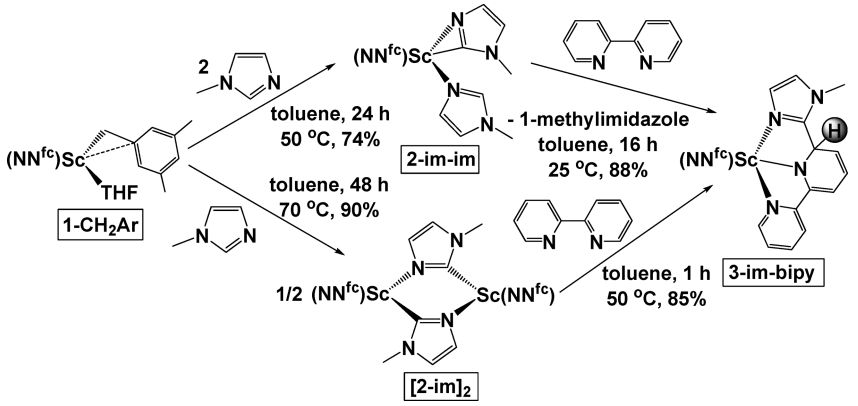

previously reported compound **2-py^{Et}-py**, which contains a Sc-CH_2CH_2-pyridine motif,[27] toward 3-methylisoquinoline was also investigated. Consequently (eq 2), the coupling product **6-py^{Et}-iqn^{Me}** (Figure 4) was formed by the addition of 1 equiv of 3-methylisoquinoline to **2-py^{Et}-py** after heating to 70 °C for 16 h. It is interesting to note that by effecting the coupling with 3-methylisoquinoline, this substrate was preferred to pyridine, which was present in the reaction mixture since it had to decoordinate from **2-py^{Et}-py**. Despite the presence of two different pyridines, **6-py^{Et}-iqn^{Me}** was isolated in 86% yield and no other products were observed in the ^{1}H NMR spectrum of the reaction mixture. As was the case for **5-lut-iqn^{Me}**, prolonged heating of **6-py^{Et}-iqn** showed no observable change by ^{1}H NMR spectroscopy.

In an attempt to determine whether the nucleophilic attack of an η^2-imidazolyl ligand is capable of leading to the ring-opening of other N-heterocycles and generalize the ring-opening reaction of 1-methylimidazole previously reported by our group (Scheme 1),[29] efforts were made to prepare solvates and coupled products starting from a (NN^{fc})Sc(η^2-N,C-imidazolyl) fragment. Although the 1-methylimidazole solvate of the η^2-imidazolyl complex Sc(fc[NSi^{t}BuMe$_2$]$_2$)(η^2-N,C-2-(1-methylimidazolyl)(1-methylimidazole), **2-im-im**, was isolated (Scheme 6), all attempts to isolate a THF or nonchelating-pyridine solvate of (NN^{fc})Sc(η^2-N,C-imidazolyl) resulted in the formation of [(NN^{fc})Sc(μ^2,κ^2-N,C-2-(1-methylimidazolyl)]$_2$, $[\mathbf{2\text{-}im}]_2$ (Scheme 6), in which the two scandium centers are bridged by two imidazolyl ligands. The complex $[\mathbf{2\text{-}im}]_2$ was characterized by X-ray crystallography (Figure 5) and features an iron−scandium distance of 3.081 Å, which is shorter than the corresponding one in **1-CH_2Ar** (3.1582(17) Å).[25] The iron−scandium distance was previously correlated by us to the electrophilicity of the scandium center in alkyl complexes: the shorter the distance, the more electrophilic the scandium center.[25] However, the different ligands in $[\mathbf{2\text{-}im}]_2$ (bridging imidazolyl versus alkyl) and the insolubility of $[\mathbf{2\text{-}im}]_2$ invalidate a direct comparison between the reactivity of **1-CH_2Ar** and that of $[\mathbf{2\text{-}im}]_2$.

Although neither **2-im-im** nor $[\mathbf{2\text{-}im}]_2$ reacted with pyridines, both complexes reacted with 2,2′-bipyridine at 50 °C and yielded the bright red-orange coupled product **3-im-bipy** (Scheme 6, Figure 5). Attempts to study a further transformation of **3-im-bipy** by prolonged heating (72 h at 70 °C) were not successful (no difference was observed by ^{1}H NMR spectroscopy).

Conclusions

We have shown that the C−C coupling between η^2-N,C-pyridyl and pyridine ligands coordinated to a group 3 metal center supported by a ferrocene-diamide ligand is rather general; in fact, the list of complexes reported herein is by no means exhaustive. The observed coupling can be rationalized by invoking standard reactivity arguments: the pyridyl fragments coordinated to early transition metals possess a polarized metal−carbon bond, rendering the carbon center

nucleophilic. Meanwhile, the *ortho* positions of coordinated pyridine ligands contain an electrophilic carbon center, as seen in pyridinium salts. A report by Cronin et al. showed that phenanthridinium salts reacted with amines: nucleophilic attack of a primary amine on the iminium moiety of the heteroaromatic ring and cyclization to form a five-membered ring, followed by hydride loss, yielded a rearomatized phenanthridinium derivative.[53,54] Three factors were found to influence the outcome of the C−C coupling reactions: (1) the use of bulky *ortho* substituents on the η^2-N,C-pyridyl ligands promotes the coupling of the two heterocycles; (2) the use of chelating substrates is beneficial; (3) fused aromatic rings on the coupling partner have an accelerating effect.

The coupling and dearomatization reaction is not restricted to η^2-N,C-pyridyl fragments, and it can proceed from methylene or ethylene groups bound to the metal center and connected to a pyridine ligand. Also, the reaction is not limited to the nucleophilic attack of η^2-N,C-pyridyl ligands, and it can be accomplished by the attack of η^2-N,C-imidazolyl ligands on bipy. Unfortunately, reactions with monopyridines could be achieved neither from **[2-im]$_2$**, likely because of its high stability and insolubility, nor from **2-im-im**, because of the lower Lewis basicity of pyridines than that of 1-methylimidazole that does not allow imidazole displacement. Given that in HDN catalysis the dearomatization of N-heterocycles precedes ring-opening and nitrogen removal, the dearomatization reactions presented herein are relevant to the modeling of HDN processes, although the ring-opening of pyridines remains a tantalizing but difficult goal.

Experimental Section

All experiments were performed under a dry-nitrogen atmosphere using standard Schlenk techniques or an MBraun inert-gas glovebox. Solvents were purified using a two-column, solid-state purification system by the method of Grubbs[55] and transferred to the glovebox without exposure to air. NMR solvents were obtained from Cambridge Isotope Laboratories, degassed, and stored over activated molecular sieves prior to use. K(CH$_2$Xy-3,5), KCH$_2$Ph, **1-CH$_2$Ar**, **1^{Y}-CH$_2$Ph**, and **1^{La}-CH$_2$Ph** were prepared following published procedures.[25,28,56] The aromatic heterocycles were distilled or recrystallized before use; all other materials were used as received. ^{1}H NMR spectra were recorded on Bruker300, Bruker500, or Bruker600 spectrometers (work supported by the NSF grants CHE-9974928 and CHE-0116853) at room temperature in C_6D_6 unless otherwise specified. Chemical shifts are reported with respect to internal solvent, 7.16 ppm (C_6D_6). CHN analyses were performed by UC Berkeley Micro-Mass facility, College of Chemistry, University of California, Berkeley, CA, and by Midwest Microlab, LLC, Indianapolis, IN.

Synthesis of 2-py^{Si}. 1-CH$_2$Ar (500 mg, 0.737 mmol) was combined with 1 equiv of 2-trimethylsilylpyridine (110 mg, 0.758 mmol) in toluene and stirred for 16 h at 35 °C. The volatiles were removed under reduced pressure, and the resulting yellow solid was washed with hexanes (2 mL), extracted in toluene, and filtered through Celite. Yield: 450 mg, 86%. ^{1}H NMR (500 MHz, C_6D_6), δ (ppm): 7.77 (d, 1H, py), 7.27−7.21 (m, 2H, py), 4.20 (br s, 2H, fc-C*H*), 4.17 (s, 4H, OC*H*$_2$CH$_2$), 4.11 (br s, 2H, fc-C*H*), 3.76 (br s, 2H, fc-C*H*), 3.28 (br s, 2H, fc-C*H*), 1.50 (s, 4H, OCH$_2$C*H*$_2$), 0.90 (s, 18H, SiC(C*H*$_3$)$_3$), 0.48 (s, 9H, Si(C*H*$_3$)$_3$), −0.00 and −0.31 (s, 12H, Si(C*H*$_3$)$_2$). ^{13}C NMR (126 MHz, C_6D_6), δ (ppm): 162.3 (py), 132.0 (py), 129.6 (py), 128.8 (py), 101.2 (fc-*C*N), 72.7 (O*C*H$_2$CH$_2$), 67.9 (fc-*C*H), 66.5 (fc-*C*H), 27.8 (SiC(*C*H$_3$)$_3$), 25.5 (OCH$_2$*C*H$_2$), 20.4 (Si*C*(CH$_3$)$_3$), −0.7 (Si*C*H$_3$), −2.3 and −3.2 (Si(*C*H$_3$)$_2$). Anal. Calcd (%) for $C_{34}H_{58}FeN_3OSi_2Sc$: C, 57.52; H, 8.23; N, 5.92. Found: C, 57.41; H, 8.27; N, 5.91.

Synthesis of 2-lut. 1-CH$_2$Ar (500 mg, 0.737 mmol) was combined with 1.03 equiv of 2,6-lutidine (81.3 mg, 0.758 mmol) in toluene and stirred for 16 h at 50 °C. The volatiles were removed under reduced pressure, and the resulting yellow solid was washed with hexanes (2 mL), extracted in toluene, and filtered through Celite. Yield: 485 mg, 99%. ^{1}H NMR (500 MHz, C_6D_6), δ (ppm): 6.98 (t, 1H, lut-C*H*), 6.84 (d, 1H, lut-C*H*), 6.17 (d, 1H, lut-C*H*), 4.09 (s, 4H, fc-C*H*), 3.96 (s, 4H, OC*H*$_2$CH$_2$), 3.34 (s, 4H, fc-C*H*), 2.39 (s, 2H, Sc-C*H*$_2$), 2.35 (s, 3H, lut-C*H*$_3$), 1.38 (s, 4H, OCH$_2$C*H*$_2$), 0.94 (s, 18H, SiC(C*H*$_3$)$_3$), 0.17 (s, 12H, Si(C*H*$_3$)$_2$). ^{13}C NMR (126 MHz, C_6D_6), δ (ppm): 169.8 (lut), 155.0 (lut), 137.6 (lut), 120.4 (lut), 112.8 (lut), 101.5 (fc-*C*N), 71.8 (O*C*H$_2$CH$_2$), 67.9 (fc-*C*H), 67.6 (fc-*C*H), 49.9 (Sc-*C*H$_2$), 27.9 (SiC(*C*H$_3$)$_3$), 25.1 (OCH$_2$*C*H$_2$), 24.3 (lut-*C*H$_3$), 20.4 (Si*C*(CH$_3$)$_3$), −2.3 (Si(*C*H$_3$)$_2$). Anal. Calcd (%) for $C_{33}H_{54}FeN_3OSi_2Sc$: C, 59.53; H, 8.17; N, 6.31. Found: C, 59.62; H, 8.35; N, 6.31.

Synthesis of 2-bqn. 1-CH$_2$Ar (400 mg, 0.589 mmol) was combined with 1 equiv of 7,8-benzoquinoline (105.6 mg, 0.589 mmol) in toluene and stirred for 16 h at 25 °C. The volatiles were removed under reduced pressure, and the resulting yellow solid was washed with hexanes (2 mL), extracted in toluene, and filtered through Celite. Yield: 351 mg, 81%. ^{1}H NMR (500 MHz, C_6D_6), δ (ppm): 9.56 (d, 1H, bqn), 8.15 (d, 1H, bqn), 7.87 (d, 1H, bqn), 7.61, (t, 1H, bqn), 7.52 (d, 1H, bqn), 7.43, (t, 1H, bqn), 7.41 (d, 1H, bqn), 4.39 (s, 2H, fc-C*H*), 4.25 (s, 4H, OC*H*$_2$CH$_2$), 4.18 (s, 2H, fc-C*H*), 4.05 (s, 2H, fc-C*H*), 3.33 (s, 2H, fc-C*H*), 1.52 (s, 4H, OCH$_2$C*H*$_2$), 0.74 (s, 18H, SiC(C*H*$_3$)$_3$), −0.27 and −0.33 (s, 12H, Si(C*H*$_3$)$_2$). ^{13}C NMR (126 MHz, C_6D_6), δ (ppm): 143.0 (bqn), 134.3 (bqn), 133.6 (bqn), 129.3 (bqn), 128.6 (bqn), 127.0 (bqn), 126.7 (bqn), 126.4 (bqn), 126.2 (bqn), 125.8 (bqn), 101.6 (fc-*C*-N), 72.7 (O*C*H$_2$CH$_2$), 68.6 (fc-*C*H), 68.1 (fc-*C*H), 67.3 (fc-*C*H), 66.8 (fc-*C*H), 27.5 (SiC(*C*H$_3$)$_3$), 25.5 (OCH$_2$*C*H$_2$), 20.1 (Si*C*(CH$_3$)$_3$), −2.4 and −3.0 (Si(*C*H$_3$)$_2$). Anal. Calcd (%) for $C_{39}H_{54}FeN_3OSi_2Sc$: C, 63.48; H, 7.37; N, 5.69. Found: C, 63.12; H, 7.19; N, 5.50.

Synthesis of 2-acr. 1-CH$_2$Ar (300 mg, 0.442 mmol) was combined with 1.05 equiv of acridine (83.1 mg, 0.464 mmol) in toluene (10 mL) and stirred for 16 h at 70 °C. The volatiles were removed under reduced pressure, and the resulting yellow solid was washed with hexanes (2 mL), extracted in toluene, and filtered through Celite. Yield: 248 mg, 76%. ^{1}H NMR (600 MHz, C_6D_6), δ (ppm): 8.59 (d, 1H, acr), 8.28 (s, 1H, acr), 8.25 (d, 1H, acr), 7.68 (t, 1H, acr), 7.06 (t, 2H, acr), 7.47 (t, 1H, acr), 7.12 (t, 1H, acr), 4.36 (s, 2H, fc-C*H*), 4.31 (s, 4H, OC*H*$_2$CH$_2$), 4.18 (s, 2H, fc-C*H*), 4.04 (s, 2H, fc-C*H*), 3.31 (s, 2H, fc-C*H*), 1.59 (s, 4H, OCH$_2$C*H*$_2$), 0.74 (s, 18H, SiC(C*H*$_3$)$_3$), −0.37 and −0.41 (s, 12H, Si(C*H*$_3$)$_2$). ^{13}C NMR (150 MHz, C_6D_6), δ (ppm): 160.0 (acr), 145.1 (acr), 138.2 (acr), 136.5 (acr), 130.0 (acr), 129.1 (acr), 127.5 (acr), 127.3 (acr), 126.3 (acr), 126.1 (acr), 125.0 (acr), 123.8 (acr), 101.6 (fc-*C*N), 72.2 (O*C*H$_2$CH$_2$), 69.0 (fc-*C*H), 68.1 (fc-*C*H), 67.0 (fc-*C*H), 66.9 (fc-*C*H), 27.6 (SiC(*C*H$_3$)$_3$), 25.5 (OCH$_2$*C*H$_2$), 20.3 (Si*C*(CH$_3$)$_3$), −2.2 and −2.8 (Si(*C*H$_3$)$_2$). Anal. Calcd (%) for $C_{39}H_{54}FeN_3OSi_2Sc$: C, 63.48; H, 7.37; N, 5.69; Found: C, 64.09; H, 7.45; N, 5.72.

Synthesis of 3-py^{Ph}-phan. 2-py^{Ph} (120 mg, 0.168 mmol) was dissolved in toluene (2 mL) and combined with a solution of phenanthridine (30.1 mg, 0.168 mmol) in toluene (1 mL). The

(53) Parenty, A. D. C.; Smith, L. V.; Pickering, A. L.; Long, D.-L.; Cronin, L. *J. Org. Chem.* **2004**, *69*, 5934–5946.
(54) Parenty, A. D. C.; Song, Y.-F.; Richmond, C. J.; Cronin, L. *Org. Lett.* **2007**, *9*, 2253–2256.
(55) Pangborn, A. B.; Giardello, M. A.; Grubbs, R. H.; Rosen, R. K.; Timmers, F. J. *Organometallics* **1996**, *15*, 1518–1520.
(56) Miller, K. L.; Williams, B. N.; Benitez, D.; Carver, C. T.; Ogilby, K. R.; Tkatchouk, E.; Goddard, W. A.; Diaconescu, P. L. *J. Am. Chem. Soc.* **2010**, *132*, 342−355.

solution was allowed to stand at room temperature for 2 h without stirring. Analytically pure red crystals were collected directly from the reaction mixture. Yield: 106.3 mg, 77%. ^{1}H NMR (600 MHz, C_4D_8O), δ (ppm): 8.35 (t, 1H, py^{Ph}-phan), 8.01 (d, 1H, py^{Ph}-phan), 7.96 (d, 2H, py^{Ph}-phan), 7.91, (d, 1H, py^{Ph}-phan), 7.79 (d, 1H, py^{Ph}-phan), 7.74, (d, 1H, py^{Ph}-phan), 7.65−7.58 (m, 3H, py^{Ph}-phan), 7.29 (t, 1H, py^{Ph}-phan), 7.19 (t, 1H, py^{Ph}-phan), 7.16−7.12 (m, 2H, py^{Ph}-phan), 7.02 (t, 1H, py^{Ph}-phan), 6.70 (d, 1H, py^{Ph}-phan), 6.65 (t, 1H, py^{Ph}-phan), 5.96 (s, 1H, sp^3-C*H*), 4.41 (br s, 2H, fc-C*H*), 3.96 (s, 2H, fc-C*H*), 3.52 (br s, 1H, fc-C*H*), 3.19 (br s, 1H, fc-C*H*), 2.31 (s, 2H, fc-C*H*), 0.44 and 0.29 (br s, 18H, SiC(CH_3)$_3$), −0.21, −0.26, −0.64, and −0.73 (s, 12H, Si(CH_3)$_2$). The limited solubility of **3-py^{Ph}-phan** prevented the collection of its ^{13}C NMR spectrum. Anal. Calcd (%) for $C_{46}H_{55}FeN_4ScSi_2$: C, 67.30; H, 6.75; N, 6.83. Found: C, 67.36; H, 6.75; N, 6.87.

Synthesis of 3-py^{Ph}-bipy. 2-py^{Ph} (120 mg, 0.168 mmol) was combined with 1 equiv of 2,2′-bipyridine (26.3 mg, 0.168 mmol) in toluene (10 mL) and stirred overnight at 50 °C. The volatiles were removed under reduced pressure, and the resulting orange-brown solid was washed with hexanes, extracted in toluene, and filtered through Celite. Yield: 114.2 mg, 85.2% as two crops from toluene/*n*-pentane. ^{1}H NMR (500 MHz, C_6D_6), δ (ppm): 9.32 (d, 1H, py^{Ph}-bipy), 7.77 (d, 2H, py^{Ph}-bipy), 7.40 (d, 1H, py^{Ph}-bipy), 7.35 (t, 2H, py^{Ph}-bipy), 7.05 (t, 1H, py^{Ph}-bipy), 7.02 (t, 1H, py^{Ph}-bipy), 6.90 (t, 1H, py^{Ph}-bipy), 6.68 (d, 1H, py^{Ph}-bipy), 6.54 (t, 1H, py^{Ph}-bipy), 6.42 (t, 1H, py^{Ph}-bipy), 6.13 (d, 1H, sp^3-C*H*), 5.70 (s, 1H, py^{Ph}-bipy), 5.33 (dd, 1H, py^{Ph}-bipy), 4.29, 4.22, 3.96, 3.84, 3.69, 3.47, 3.34, and 1.85 (s, 8H, fc-C*H*), 0.85 and 0.73 (br s, 18H, SiC(CH_3)$_3$), 0.37, 0.28, −0.23, and −0.26 (s, 12H, Si(CH_3)$_2$). ^{13}C NMR (150 MHz, C_6D_6), δ (ppm): 168.2 (py^{Ph}-bipy), 160.1 (py^{Ph}-bipy), 159.9 (py^{Ph}-bipy), 152.2 (py^{Ph}-bipy), 148.7 (py^{Ph}-bipy), 140.6 (py^{Ph}-bipy), 138.4 (py^{Ph}-bipy), 137.3 (py^{Ph}-bipy), 130.1 (py^{Ph}-bipy), 129.3 (py^{Ph}-bipy), 129.1 (py^{Ph}-bipy), 124.9 (py^{Ph}-bipy), 120.5 (py^{Ph}-bipy), 119.6 (py^{Ph}-bipy), 114.0 (py^{Ph}-bipy), 100.2 (fc-*C*N), 99.0 (fc-*C*N), 98.2 (py^{Ph}-bipy), 70.6 (fc-*C*H), 70.1 (fc-*C*H), 69.3 (fc-*C*H), 68.6 (fc-*C*H), 67.8 (py^{Ph}-bipy), 66.2 (fc-*C*H), 65.7 (fc-*C*H), 65.6 (fc-*C*H), 64.4 (py^{Ph}-bipy), 27.8 and 27.6 (SiC(*C*H$_3$)$_3$), 20.4 and 20.1 (Si*C*(CH$_3$)$_3$), −1.1, −2.7, −3.0, and −4.4 (Si(*C*H$_3$)$_2$). Anal. Calcd (%) for $C_{43}H_{54}FeN_5ScSi_2$: C, 64.73; H, 6.82; N, 8.72. Found: C, 64.97; H, 6.74; N, 8.76.

Synthesis of 3-py^{Si}-iqn^{Me}. 2-py^{Si} (200 mg, 0.293 mmol) was combined with 3-methylisoquinoline (40.3 mg, 0.293 mmol) in toluene (10 mL) and stirred for 1 h at room temperature. The volatiles were removed under reduced pressure, and the resulting red solid was washed with hexanes, extracted in toluene, and filtered through Celite. Yield: 219 mg, 99% (precipitate from toluene). ^{1}H NMR (500 MHz, C_6D_6), δ (ppm): 7.25−7.19 (m, 2H, py^{Si}-iqn^{Me}), 7.08−6.99 (m, 4H, py^{Si}-iqn^{Me}), 6.67 (d, 1H, py^{Si}-iqn^{Me}), 5.84 (s, 1H, sp^3-C*H*) 5.66 (s, 1H, py^{Si}-iqn^{Me}), 4.26 (s, 1H, fc-C*H*), 4.19 (s, 1H, fc-C*H*), 4.04 (s, 1H, fc-C*H*), 3.99 (s, 1H, fc-C*H*), 3.48 (s, 1H, fc-C*H*), 3.40 (s, 1H, fc-C*H*), 3.39 (s, 1H, fc-C*H*), 3.30 (s, 1H, fc-C*H*), 2.28 (s, 3H, iqn-CH_3), 0.88 and 0.79 (s, 18H, SiC(CH_3)$_3$), 0.33 (s, 9H, Si(CH_3)$_3$), −0.05, −0.09, −0.18, and −0.37 (s, 12H, Si(CH_3)$_2$). ^{13}C NMR (126 MHz, C_6D_6), δ (ppm): 166.9 (py^{Si}-iqn^{Me}), 165.4 (py^{Si}-iqn^{Me}), 152.9 (py^{Si}-iqn^{Me}), 139.3 (py^{Si}-iqn^{Me}), 136.2 (py^{Si}-iqn^{Me}), 129.7 (py^{Si}-iqn^{Me}), 128.6 (py^{Si}-iqn^{Me}), 127.5 (py^{Si}-iqn^{Me}), 127.1 (py^{Si}-iqn^{Me}), 126.7 (py^{Si}-iqn^{Me}), 125.7 (py^{Si}-iqn^{Me}), 122.9 (py^{Si}-iqn^{Me}), 122.4 (py^{Si}-iqn^{Me}), 121.2 (py^{Si}-iqn^{Me}), 98.6 (fc-*C*N), 98.4 (fc-*C*N), 97.8 (py^{Si}-iqn^{Me}), 69.7 (fc-*C*H), 69.6 (fc-*C*H), 69.1 (fc-*C*H), 69.0 (fc-*C*H), 68.6 (fc-*C*H), 68.5 (fc-*C*H), 68.1 (fc-*C*H), 67.5 (py^{Si}-iqn^{Me}), 67.1 (fc-*C*H), 27.8 and 27.6 (SiC(*C*H$_3$)$_3$), 23.6 (iqn^{Me}), 20.3 and 19.9 (Si*C*(CH$_3$)$_3$), −0.5 (Si(*C*H$_3$)$_2$), −2.6, −3.4, and −4.3 (Si(*C*H$_3$)$_2$). Anal. Calcd (%) for $[C_{40}H_{59}FeN_4ScSi_2]_2$·toluene: C, 63.17; H, 7.68; N, 6.77. Found: C, 63.23; H, 7.86; N, 6.54.

Synthesis of 3-bqn-phan. 2-bqn (150 mg, 0.207 mmol) was dissolved in toluene (3 mL), and phenanthridine (37.1 mg, 0.207 mmol) was dissolved in *n*-pentane (2 mL). The solutions were combined and allowed to stand at room temperature for 30 min before cooling to −35 °C overnight. Analytically pure red crystals were collected the next morning. Yield: 168.7 mg, 91% as the first crop from toluene/*n*-pentane. ^{1}H NMR (600 MHz, C_6D_6), δ (ppm): 8.98 (d, 1H, bqn-phan), 8.02 (d, 1H, bqn-phan), 7.87 (d, 1H, bqn-phan), 7.69 (t, 1H, bqn-phan), 7.58 (d, 1H, bqn-phan), 7.54 (d, 1H, bqn-phan), 7.43 (d, 1H, bqn-phan), 7.34 (t, 1H, bqn-phan), 7.30 (q, 2H, bqn-phan), 7.21 (t, 2H, bqn-phan), 7.19 (d, 1H, bqn-phan), 7.02 (d, 2H, bqn-phan), 6.94 (t, 1H, bqn-phan), 6.11 (s, 1H, sp^3-C*H*), 4.47 (s, 1H, fc-C*H*), 4.21 (s, 1H, fc-C*H*), 4.03 (s, 1H, fc-C*H*), 3.87 (br s, 3H, fc-C*H*), 3.67 (s, 1H, fc-C*H*), 3.01 (s, 1H, fc-C*H*), 0.63 and 0.23 (s, 18H, SiC(CH_3)$_3$), 0.23 (br s, 6H, Si(CH_3)$_2$), 0.05 and 0.02 (s, 6H, Si(CH_3)$_2$). ^{13}C NMR (150 MHz, C_6D_6), δ (ppm): 166.2 (bqn-phan), 152.8 (bqn-phan), 145.9 (bqn-phan), 137.9 (bqn-phan), 135.2 (bqn-phan), 134.1 (bqn-phan), 130.2 (bqn-phan), 130.0 (bqn-phan), 129.8 (bqn-phan), 129.5 (bqn-phan), 129.3 (bqn-phan), 128.8 (bqn-phan), 126.7 (bqn-phan), 126.2 (bqn-phan), 125.7 (bqn-phan), 125.6 (bqn-phan), 124.7 (bqn-phan), 124.1 (bqn-phan), 124.0 (bqn-phan), 122.9 (bqn-phan), 122.3 (bqn-phan), 119.3 (bqn-phan), 118.2 (bqn-phan), 101.6 (fc-*C*N), 100.9 (fc-*C*N), 71.6, 69.7, 69.2, 68.7, 68.0, 67.9, 67.0, and 65.8 (fc-*C*H), 27.2 and 26.8 (SiC(*C*H$_3$)$_3$), 19.8 and 19.4 (Si*C*(CH$_3$)$_3$), −2.5, −2.6, −3.0, and −4.7 (Si(*C*H$_3$)$_2$). Anal. Calcd (%) for $C_{48}H_{55}FeN_4ScSi_2$·0.5(toluene): C, 69.42; H, 6.67; N, 6.29. Found: C, 69.38; H, 6.62; N, 6.24.

Synthesis of 3-acr-phan. 2-acr (222.6 mg, 0.301 mmol) was combined with 1.05 equiv of phenanthridine (56.7 mg, 0.316 mmol) in toluene (10 mL). The reaction mixture was stirred overnight at room temperature. The volatiles were removed under reduced pressure, and the resulting orange-brown solid was washed with hexanes, toluene, and diethyl ether, extracted in THF, and filtered through Celite. Yield: 222.6 mg, 87.4%. Crystals suitable for elemental analysis were obtained directly from a reaction run in diethyl ether by adding *n*-pentane to the reaction mixture and cooling to −35 °C after the reaction was complete. ^{1}H NMR (600 MHz, C_6D_6), δ (ppm): 8.75 (d, 1H, acr-phan), 8.09 (s, 1H, acr-phan), 8.01 (s, 1H, sp^3-C*H*), 7.99, (d, 1H, acr-phan), 7.94 (d, 1H, acr-phan), 7.92 (d, 1H, acr-phan), 7.57 (t, 1H, acr-phan), 7.48 (d, 1H, acr-phan), 7.39 (d, 1H, acr-phan), 7.33 (t, 1H, acr-phan), 7.27 (t, 1H, acr-phan), 7.19 (t, 1H, acr-phan), 7.18 (d, 1H, acr-phan), 7.14 (d, 2H, acr-phan), 6.83 (t, 1H, acr-phan), 6.68 (t, 1H, acr-phan), 4.32 (s, 1H, fc-C*H*), 4.23 (s, 1H, fc-C*H*), 4.13 (br s, 2H, fc-C*H*), 3.84 (s, 1H, fc-C*H*), 3.77 (s, 1H, fc-C*H*), 3.66 (s, 1H, fc-C*H*), 3.42 (s, 1H, fc-C*H*), 0.99 and 0.60 (s, 18H, SiC(CH_3)$_3$), 0.32, −0.21, −0.62, and −1.13 (s, 12H, Si(CH_3)$_2$). The limited solubility of **3-acr-phan** prevented the collection of its ^{13}C NMR spectrum. Anal. Calcd (%) for $C_{48}H_{55}FeN_4ScSi_2$: C, 68.23; H, 6.56; N, 6.63. Found: C, 68.54; H, 6.32; N, 6.53.

Synthesis of 4-py^{Ph}-bqn. 2-py^{Ph} (200 mg, 0.280 mmol) was combined with 1 equiv of 7,8-benzoquinoline (50.2 mg, 0.280 mmol) in C_6D_6 (1.5 mL). The reaction was allowed to stand at room temperature for 21 days and at 50 °C for 3 days while monitoring by ^{1}H NMR spectroscopy. When the reaction mixture contained an approximate 1:1.1 ratio of **2-py^{Ph}** to **4-py^{Ph}-bqn** and almost no **3-py^{Ph}-bqn**, the reaction was stopped. The volatiles were removed under reduced pressure, and the resulting dark green, oily solid was washed with hexanes, while the remaining orange solid was extracted with toluene and filtered through Celite. ^{1}H NMR spectroscopy showed that the green hexanes fraction contained mainly (>90%) **2-py^{Ph}**, while the orange toluene fraction contained mainly **4-py^{Ph}-bqn**. Yield: 128 mg, 55.6%. ^{1}H NMR (500 MHz, C_6D_6), δ (ppm): 7.88 (d, 1H, py^{Ph}-bqn), 7.68 (t, 3H, py^{Ph}-bqn), 7.47 (d, 1H, py^{Ph}-bqn), 7.37 (t, 1H, py^{Ph}-bqn), 7.29 (d, 1H, py^{Ph}-bqn), 7.23 (t, 2H, py^{Ph}-bqn), 7.19 (t, 1H, py^{Ph}-bqn), 7.07−7.00 (m, 3H, py^{Ph}-bqn), 6.72 (d, 1H, py^{Ph}-bqn), 5.28 (t, 1H, py^{Ph}-bqn), 4.29 (d, 2H, bqn-CH_2), 4.07, 4.01, 3.36, and 2.41 (s, 2H, fc-C*H*), 0.70 (s, 18H,

SiC(CH_3)$_3$), 0.17 and 0.11 (s, 6H, Si(CH_3)$_2$). ^{13}C NMR (126 MHz, C_6D_6), δ (ppm): 162.1 (py^{Ph}-bqn), 157.5 (py^{Ph}-bqn), 146.0 (py^{Ph}-bqn), 144.8 (py^{Ph}-bqn), 139.4 (py^{Ph}-bqn), 138.4 (py^{Ph}-bqn), 135.2 (py^{Ph}-bqn), 130.2 (py^{Ph}-bqn), 130.1 (py^{Ph}-bqn), 130.0 (py^{Ph}-bqn), 129.4 (py^{Ph}-bqn), 129.3 (py^{Ph}-bqn), 128.8 (py^{Ph}-bqn), 128.7 (py^{Ph}-bqn), 128.6 (py^{Ph}-bqn), 127.5 (py^{Ph}-bqn), 127.2 (py^{Ph}-bqn), 125.7 (py^{Ph}-bqn), 124.9 (py^{Ph}-bqn), 122.6 (py^{Ph}-bqn), 120.7 (py^{Ph}-bqn), 120.6 (py^{Ph}-bqn), 120.2 (py^{Ph}-bqn), 113.2 (py^{Ph}-bqn), 103.5 (py^{Ph}-bqn), 99.1 (fc-*C*N), 69.4, 68.4, 68.2, and 67.3 (fc-*C*H), 31.1 (bqn-CH_2), 27.5 (SiC(CH_3)$_3$), 20.0 (Si*C*(CH_3)$_3$), −3.4 and −3.6 (Si(CH_3)$_2$). Anal. Calcd (%) for $C_{46}H_{55}FeN_4ScSi_2$: C, 67.34; H, 6.75; N, 6.82. Found: C, 66.97; H, 6.81; N, 6.90.

Synthesis of 5-lut-iqn^{Me}. 2-lut (200 mg, 0.300 mmol) was combined with 3-methylisoquinoline (43.0 mg, 0.300 mmol) in toluene (10 mL) and stirred for 1 h at 25 °C. The volatiles were removed under reduced pressure, and the resulting orange solid was washed with hexanes and extracted with toluene/THF. The resulting solution was passed through Celite, concentrated, and placed in a −35 °C freezer overnight. Yield: 218.5 mg, 99%. ^{1}H NMR (500 MHz, C_6D_6), δ (ppm): 7.19 (m, 4H, lut-iqn^{Me}), 7.05 (d, 2H, lut-iqn^{Me}), 6.80 (t, 2H, lut-CH_2), 6.35 (t, 1H, lut-iqn^{Me}), 6.30 (d, 1H, lut-iqn^{Me}), 5.32 (s, 1H, lut-iqn^{Me}), 4.34 (s, 1H, fc-C*H*), 4.26 (dd, 1H, sp^3-C*H*), 4.04 (s, 1H, fc-C*H*), 3.94 (s, 1H, fc-C*H*), 3.86 (s, 1H, fc-C*H*), 3.74 (s, 1H, fc-C*H*), 3.67 (s, 1H, fc-C*H*), 3.53 (s, 1H, fc-C*H*), 3.37 (s, 1H, fc-C*H*), 2.67 (d, 1H, lut-iqn^{Me}), 2.62 (s, 3H, lut-iqn^{Me}-CH_3), 2.44 (s, 3H, lut-iqn^{Me}-CH_3), 0.94 and 0.85 (s, 18H, SiC(CH_3)$_3$), 0.20, −0.04, −0.23, and −0.32 (s, 12H, Si(CH_3)$_2$). The limited solubility of **5-lut-iqn^{Me}** prevented the collection of its ^{13}C NMR spectrum. Anal. Calcd (%) for $C_{39}H_{54}FeN_4ScSi_2$: C, 63.65; H, 7.40; N, 7.61. Found: C, 63.58; H, 7.51; N, 7.58.

Synthesis of 2^Y-pic. 1^Y-CH$_2$Ph (120.0 mg, 0.176 mmol) and 2 equiv of 2-picoline (33.2 mg, 0.356 mmol) were combined in a Schlenk tube and stirred in toluene for 17 h at 50 °C. The volatiles were removed under reduced pressure, and the resulting crude mixture was dissolved in hexanes and left at −35 °C overnight, precipitating the desired product as yellow-orange crystals and powder. Yield: 88.6% (111.9 mg, 0.156 mmol). ^{1}H NMR (500 MHz, C_6D_6), δ (ppm): 9.26 (s, 1H, pic-C*H*), 7.88 (d, 1H, pic-C*H*), 6.94 (t, 1H, pic-C*H*), 6.87 (t, 2H, pic-C*H*), 6.58 (t, 1H, pic-C*H*), 6.49 (d, 1H, pic-C*H*), 6.09 (t, 1H, pic-C*H*), 4.31 (s, 2H, fc-C*H*), 3.97 (s, 2H, fc-C*H*), 3.57 (s, 2H, fc-C*H*), 3.39 (s, 2H, fc-C*H*), 2.81 (s, 2H, pic-CH_2), 2.64 (s, 3H, pic-CH_3), 0.88 (s, 18H, SiC(CH_3)$_3$), −0.01 (s, 6H, Si(CH_3)$_2$), −0.17 (s, 6H, Si(CH_3)$_2$). ^{13}C NMR (126 MHz, C_6D_6), δ (ppm): 168.0, 158.8, 150.6, 147.2, 138.4, 136.3, 124.7, 120.9, 120.0, and 108.9 (pic-*C*H), 104.9 (fc-*C*N), 68.5, 68.3, 67.1, 64.0, and 53.3 (fc-*C*H), 53.2 (pic-*C*H$_2$), 27.0 (SiC(*C*H$_3$)$_3$), 23.7 (pic-CH$_3$), 19.8 (SiC(*C*H$_3$)$_3$), −3.60 (Si(*C*H$_3$)$_2$). Anal. Calcd (%) for $C_{34}H_{51}N_4FeYSi_2$: C, 56.98; H, 7.17; N, 7.82. Found: C, 56.88; H, 7.09; N, 7.56.

Synthesis of 2^{La}-pic. 1^{La}-CH$_2$Ph (535.7 mg, 0.719 mmol) and 2 equiv of 2-picoline (134.0 mg, 1.439 mmol) were dissolved in toluene and cooled to −78 °C. The two solutions were combined and allowed to stir at room temperature for 2 h. The volatiles were removed under reduced pressure, the resulting mixture was dissolved in hexanes, and the solution was filtered through Celite, concentrated, and placed in a −35 °C freezer overnight. The desired product precipitated as yellow-orange crystals and powder. Yield: 89.6% (494.2 mg, 0.645 mmol). ^{1}H NMR (500 MHz, C_6D_6), δ (ppm): 8.94 (s, 1H, pic-C*H*), 7.80 (d, 1H, pic-C*H*), 6.88 (t, 1H, pic-C*H*), 6.83 (t, 1H, pic-C*H*), 6.79 (t, 1H, pic-C*H*), 6.55 (t, 1H, pic-C*H*), 6.47 (d, 1H, pic-C*H*), 5.97 (t, 1H, pic-C*H*), 4.15 (s, 4H, fc-C*H*), 3.38 (s, 4H, fc-C*H*), 3.03 (s, 2H, pic-CH_2), 2.52 (s, 3H, pic-CH_3), 0.87 (s, 18H, SiC(CH_3)$_3$), −0.01 (s, 12H, Si(CH_3)$_2$). ^{13}C NMR (126 MHz, C_6D_6), δ (ppm): 164.1, 158.5, 149.5, 147.0, 139.0, 135.5, 125.1, 121.7, 120.2, and 106.9 (pic-*C*H), 105.2(fc-*C*N), 66.5 (fc-*C*H), 62.1 (pic-*C*H$_2$), 27.2 (SiC(*C*H$_3$)$_3$), 22.8 (pic-*C*H$_3$), 20.2 (Si*C*(CH$_3$)$_3$), −3.71 (Si(*C*H$_3$)$_2$). Anal. Calcd (%) for $C_{34}H_{51}N_4FeLaSi_2$: C, 53.26; H, 6.70; N, 7.31. Found: C, 53.26; H, 6.52; N, 6.92.

Synthesis of 5^Y-pic-iqn^{Me}. 2^Y-pic (132.1 mg, 0.184 mmol) and 2 equiv of 3-methylisoquinoline (54.9 mg, 0.383 mmol) were combined in a capped 20 mL scintillation vial and stirred for 2 h in toluene at room temperature. The volatiles were removed under reduced pressure, and the resulting crude mixture was dissolved in *n*-pentane and left at −35 °C overnight to precipitate **5^Y-pic-iqn^{Me}**. Yield: 49.6% (85.8 mg, 0.0942 mmol) of a red-orange powder. ^{1}H NMR (500 MHz, C_6D_6), δ (ppm): 9.94 (s, 1H, aromatic-C*H*), 8.87 (d, 1H, aromatic-C*H*), 7.71 (d, 1H, aromatic-C*H*), 7.27, 7.23, 7.18, 7.09, 7.05, 7.01, 6.87 (m, 8H, aromatic-C*H*), 6.61 (t, 1H, aromatic-C*H*), 6.45 (d, 1H, aromatic-C*H*), 6.02 (d, 1H, aromatic-C*H*), 5.26 (s, 1H, iqn-NC(CH$_3$)C*H*), 4.35 (dd, 1H, NC*H*CH$_2$), 4.06 and 3.78 (m, 8H, fc-C*H*), 2.83 (s, 3H, NC(CH_3)), 2.52 (d, 2H, pic-CH_2), 1.84 (s, 3H, iqn-CH_3), 1.01 (s, 18H, SiC(CH_3)$_3$), 0.12 (br d, 12H, Si(CH_3)$_2$). ^{13}C NMR (126 MHz, C_6D_6), δ (ppm): 163.9, 153.8, 151.4, 150.1, 147.1, 138.6, 138.1, 136.7, 131.0, 128.3, 128.1, 127.2, 126.6, 126.1, 125.7, 125.0, 121.7, 120.1, 119.9, and 119.7 (aromatic-*C*H), 92.0, 67.2, 65.9, and 64.2 (fc-*C*H), 55.9 (NC(*C*H$_3$)), 43.8 (pic-*C*H$_2$), 27.8 (SiC(*C*H$_3$)$_3$), 25.3 (iqn*-*C*H$_3$), 24.3 (iqn-*C*H$_3$), 20.5 (SiC(*C*H$_3$)$_3$), −1.7 and −4.5 (Si(*C*H$_3$)$_2$). Anal. Calcd (%) for $C_{48}H_{63}N_5FeYSi_2$: C, 63.29; H, 6.97; N, 7.69. Found: C, 62.46; H, 6.79; N, 7.76.

Synthesis of 5^{La}-pic-iqn^{Me}. 2^{La}-pic (486.7 mg, 0.635 mmol) and 2 equiv of 3-methylisoquinoline (181.8 mg, 1.269 mmol) were dissolved in toluene and cooled to −78 °C. The two solutions were combined, and the mixture was stirred at room temperature for 1 h. The volatiles were removed under reduced pressure, and the resulting crude mixture was washed with hexanes. The solid was dissolved in toluene, and the solution was filtered through Celite, layered with *n*-pentane, and placed in a −35 °C freezer overnight to precipitate **5^{La}-pic-iqn^{Me}**. Yield: 67.9% (413.6 mg, 0.413 mmol) of red-orange crystals. ^{1}H NMR (500 MHz, C_6D_6), δ (ppm): 9.80 (s, 1H, aromatic-C*H*), 8.77 (d, 1H, aromatic-C*H*), 7.62 (d, 1H, aromatic-C*H*), 7.33 (d, 1H, aromatic-C*H*), 7.24 (t, 1H, aromatic-C*H*), 7.10 (t, 1H, aromatic-C*H*), 7.02 (m, 2H, aromatic-C*H*), 6.90 (t, 1H, aromatic-C*H*), 6.81 (s, 1H, aromatic-C*H*), 6.66 (t, 1H, aromatic-C*H*), 6.51 (d, 1H, aromatic-C*H*), 5.98 (d, 1H, aromatic-C*H*), 5.17 (s, 1H, iqn-NC(CH$_3$)C*H*), 4.26 (dd, 1H, NC*H*CH$_2$), 4.10 (s, 2H, fc-C*H*), 3.96 (s, 2H, fc-C*H*), 3.63 (s, 2H, fc-C*H*), 3.29 (s, 1H, fc-C*H*), 2.78 (s, 3H, NC(CH_3)), 2.66 (d, 2H, pic-CH_2), 1.86 (s, 3H, iqn-CH_3), 1.00 (s, 18H, SiC(CH_3)$_3$), 0.13 (br s, 12H, Si(CH_3)$_2$). ^{13}C NMR (126 MHz, C_6D_6), δ (ppm): 164.5, 153.3, 150.9, 150.6, 146.5, 138.9, 138.7, 137.3, 132.0, 128.6, 127.5, 127.4, 126.7, 126.6, 126.1, 125.4, 121.7, 120.9, 120.5, and 120.2 (aromatic-*C*H), 107.3 (fc-*C*N), 91.2 and 66.7 (fc-*C*H), 56.2 (NC(*C*H$_3$)), 44.8 (pic-*C*H$_2$), 28.0 (SiC(*C*H$_3$)$_3$), 24.0 (iqn-*C*H$_3$), 20.9 (Si*C*(CH$_3$)$_3$), −1.6 (Si(*C*H$_3$)$_2$). Anal. Calcd (%) for $C_{48}H_{63}N_5FeLaSi_2$: C, 60.06; H, 6.51; N, 7.30. Found: C, 59.97; H, 6.65; N, 7.23.

Synthesis of 6-py^{Et}-iqn^{Me}. 2-py^{Et}-py (133.3 mg, 0.194 mmol) was combined with 1 equiv of 3-methylisoquinoline (27.7 mg, 0.194 mmol) in C_6D_6 (1 mL). The reaction mixture was heated to 70 °C for 16 h. The volatiles were removed under reduced pressure, the resulting yellow solid was washed with hexanes and extracted in toluene, and the solution was filtered through Celite. Yield: 122.7 mg, 86% (precipitate from toluene). ^{1}H NMR (600 MHz, C_6D_6), δ (ppm): 8.58 (d, 1H, py^{Et}-iqn^{Me}), 7.18 (m, 2H, py^{Et}-iqn^{Me}), 7.09 (d, 1H, py^{Et}-iqn^{Me}), 7.04, (t, 1H, py^{Et}-iqn^{Me}), 6.89 (t, 1H, py^{Et}-iqn^{Me}), 6.56 (t, 1H, py^{Et}-iqn^{Me}), 6.49 (d, 1H, py^{Et}-iqn^{Me}), 5.57 (dd, 1H, py^{Et}-iqn^{Me}), 5.46 (s, 1H, py^{Et}-iqn^{Me}), 4.12 (s, 1H, fc-C*H*), 3.98 (s, 1H, fc-C*H*), 3.96 (s, 1H, fc-C*H*), 3.09 (s, 1H, fc-C*H*), 3.77 (s, 1H, fc-C*H*), 3.63 (m, 1H, CH_2), 3.53 (s, 1H, fc-C*H*), 3.48 (s, 1H, fc-C*H*), 3.46 (s, 1H, fc-C*H*), 2.68 (m, 1H, CH_2), 2.53 (s, 3H, iqn-CH_3), 2.63 (m, 1H, CH_2), 1.53 (m, 1H, CH_2), 0.93 and 0.92 (s, 18H, SiC(CH_3)$_3$), 0.06, 0.05, −0.11, and −0.39 (s, 12H, Si(CH_3)$_2$). ^{13}C NMR (150 MHz, C_6D_6), δ (ppm): 163.0 (py^{Et}-iqn^{Me}), 149.5 (py^{Et}-iqn^{Me}), 148.5

(py^{Et}-iqn^{Me}), 140.6 (py^{Et}-iqn^{Me}), 136.4 (py^{Et}-iqn^{Me}), 131.0 (py^{Et}-iqn^{Me}), 127.2 (py^{Et}-iqn^{Me}), 125.7 (py^{Et}-iqn^{Me}), 125.5 (py^{Et}-iqn^{Me}), 122.6 (py^{Et}-iqn^{Me}), 121.9 (py^{Et}-iqn^{Me}), 106.8 and 105.3 (fc-*C*N), 94.7 (py^{Et}-iqn^{Me}), 70.6, 69.6, 69.2, 68.8, 68.5, 68.0, 66.9, and 65.8 (fc-*C*H), 53.0 (py^{Et}-iqn^{Me}), 35.5 and 32.6 ((CH_2)$_2$), 28.4 and 28.0 (SiC(CH_3)$_3$), 24.9 (iqn-CH_3), 20.5 and 20.4 (Si*C*(CH_3)$_3$), −1.4, −1.7, −2.8, and −3.3 (Si(CH_3)$_2$). Anal. Calcd (%) for $C_{39}H_{55}FeN_4ScSi_2$: C, 63.57; H, 7.52; N, 7.60. Found: C, 63.25; H, 7.41; N, 7.32.

Synthesis of [2-im]$_2$. 1-CH_2Ar (200 mg, 0.295 mmol) was combined with 0.95 equiv of 1-methylimidazole (23.0 mg, 0.280 mmol) in toluene (5 mL) and stirred at 70 °C for 48 h. The volatiles were removed under reduced pressure, the resulting yellow solid was washed with hexanes and extracted in toluene, and the solution was filtered through Celite. Yield: 150.7 mg, 90%. ^{1}H NMR (500 MHz, C_6D_6), δ (ppm): 7.59 (d, 2H, im), 6.44 (d, 2H, im), 4.23, 3.88, 3.81, and 3.79 (s, 4H each, fc-C*H*), 3.77 (s, 6H, im-CH_3), 0.99 (s, 36H, SiC(CH_3)$_3$), −0.08 and −0.11 (s, 12H each, Si(CH_3)$_2$). The limited solubility of **[2-im]$_2$** prevented the collection of its ^{13}C spectrum. Anal. Calcd (%) for $C_{52}H_{86}Fe_2N_8Sc_2Si_4$: C, 54.92; H, 7.62; N, 9.85. Found: C, 54.86; H, 7.51; N, 9.54.

Synthesis of 2-im-im. 1-CH_2Ar (200 mg, 0.295 mmol) was combined with 1.99 equiv of 1-methylimidazole (48 mg, 0.586 mmol) in toluene (8 mL) and heated to 50 °C for 24 h. The volatiles were removed under reduced pressure, the resulting solid was washed with a small (ca. 2 mL) amount of cold hexanes and extracted with hexanes, and the solution was filtered through Celite. Yield: 142 mg, 74.1%. ^{1}H NMR (500 MHz, C_6D_6), δ (ppm): 7.80 (br s, 1H, im), 7.45 (br s, 1H, im), 7.23(s, 1H, im), 6.92 (s, 1H, im), 5.95 (s, 1H, im), 4.18 (s, 4H, fc-C*H*), 3.59 (br s, 4H, fc-C*H*), 3.42 (s, 3H, im-CH_3), 2.35 (s, 3H, im-CH_3), 1.01 (s, 18H, SiC(CH_3)$_3$), 0.06 (s, 12H, Si(CH_3)$_2$). ^{13}C NMR (126 MHz, C_6D_6), δ (ppm): 200.8 (im), 140.0 (im), 130.0 (im), 126.8 (im), 124.8 (im), 119.8 (im), 103.3 (fc-*C*N), 67.5 and 67.2 (fc-*C*H), 36.0, 32.6, and 28.5 (im-*C*H_3), 27.9 (SiC(*C*H_3)$_3$), 20.4 (Si*C*(CH_3)$_3$), −2.6 (Si(*C*H_3)$_2$). Anal. Calcd (%) for $C_{30}H_{49}FeN_6ScSi_2$: C, 55.37; H, 7.59; N, 12.91. Found: C, 55.00; H, 7.68; N, 12.61.

Synthesis of 3-im-bipy. 2-im-im (212.6 mg, 0.327 mmol) was combined with 1 equiv of 2,2′-bipyridine in toluene and stirred for 16 h at room temperature. The volatiles were removed under reduced pressure, the remaining red solid was washed with a generous portion (15 mL) of hexanes and extracted in toluene, and the solution was filtered through Celite. Yield: 209.5 mg, 88.4%. ^{1}H NMR (500 MHz, C_6D_6), δ (ppm): 8.23 (d, 1H, bipy), 7.45 (d, 1H, bipy), 6.96 (t, 1H bipy), 6.87 (s, 1H, im), 6.56 (m, 2H, bipy), 6.02 (d, 1H, bipy), 6.01 (s, 1H, im), 5.38 (s, 1H, bipy), 4.84 (d, 1H, bipy), 4.32 (s, 2H, fc-C*H*), 4.12, 4.10, and 3.68 (s, 1H, fc-C*H*), 3.56 (s, 2H, fc-C*H*), 3.54 (s, 1H, fc-C*H*), 2.65 (s, 3H, im-CH_3), 0.90 and 0.77 (s, 9H, SiC(CH_3)$_3$), 0.02, −0.07, −0.11, and −0.20 (s, 3H, Si(CH_3)$_2$). ^{13}C NMR (126 MHz, C_6D_6), δ (ppm): 159.5 (im-bipy), 155.4 (im-bipy), 153.0 (im-bipy), 145.9 (im-bipy), 137.4 (im-bipy), 129.4 (im-bipy), 125.6 (im-bipy), 121.4 (im-bipy), 121.2 (im-bipy), 120.1 (im-bipy), 103.2 (im-bipy), 102.4 and 102.1 (fc-*C*N), 96.7 (im-bipy), 68.2, 68.1, 67.9, 65.4, 65.3, and 57.5 (fc-*C*H), 32.4 (im-*C*H_3), 27.9 and 27.5 (SiC(*C*H_3)$_3$), 20.5 and 20.1 (Si*C*(CH_3)$_3$), −3.4, −3.6, and −3.7 (Si(*C*H_3)$_2$). Anal. Calcd (%) for $C_{36}H_{51}FeN_6ScSi_2$: C, 59.66; H, 7.09; N, 11.59. Found: C, 59.47; H, 7.16; N, 11.56.

X-ray Crystal Structures. X-ray quality crystals were obtained from various concentrated solutions placed in a −35 °C freezer in the glovebox. Inside the glovebox, the crystals were coated with oil (STP Oil Treatment) on a microscope slide, which was brought outside the glovebox. The X-ray data collections were carried out on a Bruker AXS single-crystal X-ray diffractometer using Mo Kα radiation and a SMART APEX CCD detector. The data were reduced by SAINTPLUS, and an empirical absorption correction was applied using the package SADABS. The structures were solved and refined using SHELXTL (Bruker 1998, SMART, SAINT, XPREP AND SHELXTL, Bruker AXS Inc., Madison, WI).[57] All atoms were refined anisotropically, and hydrogen atoms were placed in calculated positions unless specified otherwise. Tables with atomic coordinates and equivalent isotropic displacement parameters, with all the bond lengths and angles, and with anisotropic displacement parameters are listed in the cifs.

X-ray Crystal Structure of 2-lut. X-ray quality crystals were obtained from a concentrated toluene/*n*-pentane solution placed in a −35 °C freezer in the glovebox. A total of 31 986 reflections ($-13 \le h \le 13$, $-16 \le k \le 16$, $-38 \le l \le 39$) were collected at $T = 110(2)$ K with $2\theta_{max} = 56.53°$, of which 8738 were unique ($R_{int} = 0.0460$). The residual peak and hole electron density were 0.57 and −0.53 e Å^{-3}. The least-squares refinement converged normally with residuals of $R_1 = 0.0379$ and GOF = 1.032. Crystal and refinement data for **2-lut**: formula $C_{33}H_{54}N_3Si_2FeScO$, space group $P2_1/c$, $a = 10.0439(14)$ Å, $b = 12.1154(17)$ Å, $c = 29.315(4)$ Å, $\beta = 95.686(1)°$, $V = 3549.7(9)$ Å^3, $Z = 4$, $\mu = 0.696$ mm^{-1}, $F(000) = 1424$, $R_1 = 0.0544$ and $wR_2 = 0.0987$ (based on all 8738 data, $I > 2\sigma(I)$).

X-ray Crystal Structure of 3-py^{Ph}-phan. X-ray quality crystals were obtained from a concentrated C_6D_6 solution stored at room temperature in the glovebox. A total of 20 229 reflections ($-14 \le h \le 13$, $-17 \le k \le 17$, $-26 \le l \le 25$) were collected at $T = 100(2)$ K with $2\theta_{max} = 61.03°$, of which 11 291 were unique ($R_{int} = 0.0196$). The residual peak and hole electron density were 0.49 and −0.37 e Å^{-3}. The least-squares refinement converged normally with residuals of $R_1 = 0.0343$ and GOF = 1.030. Crystal and refinement data for **3-py^{Ph}-phan**: formula $C_{46}H_{55}N_4Si_2FeSc$, space group $P\bar{1}$, $a = 9.9201(8)$ Å, $b = 12.3794(10)$ Å, $c = 18.301(2)$ Å, $\alpha = 102.853(1)°$, $\beta = 101.442(1)°$, $\gamma = 103.688(1)°$, $V = 2052.7(3)$ Å^3, $Z = 2$, $\mu = 0.615$ mm^{-1}, $F(000) = 868$, $R_1 = 0.0437$ and $wR_2 = 0.0894$ (based on all 11 291 data, $I > 2\sigma(I)$).

X-ray Crystal Structure of 3-acr-phan. X-ray quality crystals were obtained from the slow diffusion of *n*-pentane into a concentrated C_6D_6 solution stored at room temperature in the glovebox. A total of 40 459 reflections ($-24 \le h \le 24$, $-18 \le k \le 18$, $-23 \le l \le 23$) were collected at $T = 100(2)$ K with $2\theta_{max} = 57.43°$, of which 11 169 were unique ($R_{int} = 0.0579$). The residual peak and hole electron density were 0.45 and −0.38 e Å^{-3}. The least-squares refinement converged normally with residuals of $R_1 = 0.0424$ and GOF = 1.005. Crystal and refinement data for **3-acr-phan**: formula $C_{48}H_{55}N_4Si_2FeSc$, space group $P2_1/c$, $a = 18.4379(15)$ Å, $b = 13.7392(11)$ Å, $c = 17.1780(14)$ Å, $\beta = 93.435(1)°$, $V = 4343.7(6)$ Å^3, $Z = 4$, $\mu = 0.583$ mm^{-1}, $F(000) = 1784$, $R_1 = 0.0735$ and $wR_2 = 0.1046$ (based on all 11 169 data, $I > 2\sigma(I)$).

X-ray Crystal Structure of 4-py^{Ph}-bqn. X-ray quality crystals were obtained from the slow diffusion of *n*-pentane into a concentrated toluene solution placed in a −35 °C freezer in the glovebox. A total of 23 249 reflections ($-12 \le h \le 12$, $-19 \le k \le 19$, $-24 \le l \le 25$) were collected at $T = 100(2)$ K with $2\theta_{max} = 55.82°$, of which 12 281 were unique ($R_{int} = 0.0410$). The residual peak and hole electron density were 0.51 and −0.36 e Å^{-3}. The least-squares refinement converged normally with residuals of $R_1 = 0.0538$ and GOF = 0.973. Crystal and refinement data for **4-py^{Ph}-bqn**: formula $C_{46}H_{55}N_4Si_2FeSc$, space group $P\bar{1}$, $a = 9.7843(15)$ Å, $b = 14.976(2)$ Å, $c = 19.261(3)$ Å, $\alpha = 90.224(2)°$, $\beta = 97.913(2)°$, $\gamma = 108.405(2)°$, $V = 2649.2(7)$ Å^3, $Z = 2$, $\mu = 0.477$ mm^{-1}, $F(000) = 868$, $R_1 = 0.0778$ and $wR_2 = 0.1612$ (based on all 12281 data, $I > 2\sigma(I)$).

X-ray Crystal Structure of 5-lut-iqn^{Me}. X-ray quality crystals were obtained from a concentrated C_6D_6 solution stored at room temperature in the glovebox. A total of 36 605 reflections ($-24 \le h \le 24$, $-17 \le k \le 17$, $-23 \le l \le 23$) were collected at $T = 100(2)$ K with $2\theta_{max} = 56.52°$, of which 9960 were unique ($R_{int} = 0.0348$). The residual peak and hole electron density were 0.52 and −0.55 e Å^{-3}. The least-squares refinement converged normally with residuals of $R_1 = 0.0361$ and GOF = 1.034. Half of a molecule of

(57) Sheldrick, G. *Acta Crystallogr. A* **2008**, *64*, 112–122.

C_6D_6 was found in the unit cell. Crystal and refinement data for **5-lut-iqn^{Me}**: formula $C_{42}H_{58}N_4Si_2FeSc$, space group $P2_1/c$, a = 18.2657(11) Å, b = 13.1113(8) Å, c = 17.9123(11) Å, β = 109.625(1)°, V = 4040.6(4) Å^3, Z = 4, μ = 0.620 mm^{-1}, $F(000)$ = 1652, R_1 = 0.0482 and wR_2 = 0.0933 (based on all 9960 data, $I > 2\sigma(I)$).

X-ray Crystal Structure of 6-py^{Et}-iqn^{Me}. X-ray quality crystals were obtained from the slow diffusion of *n*-pentane into a concentrated Et_2O solution placed at −35 °C in the glovebox. A total of 44 359 reflections ($-37 \le h \le 38$, $-19 \le k \le 19$, $-34 \le l \le 36$) were collected at T = 100(2) K with $2\theta_{max}$ = 61.73°, of which 12 957 were unique (R_{int} = 0.0446). The residual peak and hole electron density were 1.11 and −1.13 e Å^{-3}. The least-squares refinement converged normally with residuals of R_1 = 0.0487 and GOF = 1.026. A molecule of *n*-octane solvent was found in the unit cell. Crystal and refinement data for **6-py^{Et}-iqn^{Me}**: formula $C_{43}H_{63}N_4Si_2FeSc$, space group $C2/c$, a = 26.971(2) Å, b = 13.7216(12) Å, c = 25.022(2) Å, β = 109.414(1)°, V = 8733.5(13) Å^3, Z = 8, μ = 0.575 mm^{-1}, $F(000)$ = 3392, R_1 = 0.0752 and wR_2 = 0.1463 (based on all 12 957 data, $I > 2\sigma(I)$).

X-ray Crystal Structure of [2-im]$_2$. X-ray quality crystals were obtained from a concentrated C_6D_6 solution stored at room temperature in the glovebox. A total of 12 932 reflections ($-14 \le h \le 14$, $-16 \le k \le 16$, $-17 \le l \le 17$) were collected at T = 110(2) K with $2\theta_{max}$ = 56.61°, of which 7005 were unique (R_{int} = 0.0357). The residual peak and hole electron density were 1.10 and −0.77 e Å^{-3}. The least-squares refinement converged normally with residuals of R_1 = 0.0458 and GOF = 1.029. Crystal and refinement data for **[2-im]$_2$**: formula $C_{52}H_{86}N_8Si_4Fe_2Sc_2$, space group $P\bar{1}$, a = 10.821(2) Å, b = 12.104(4) Å, c = 13.158(2) Å, α = 108.410(3)°, β = 111.857(2)°, γ = 96.849(3)°, V = 1461.7(6) Å^3, Z = 1, μ = 0.831 mm^{-1}, $F(000)$ = 604, R_1 = 0.0767 and wR_2 = 0.1086 (based on all 7005 data, $I > 2\sigma(I)$).

X-ray Crystal Structure of 3-im-bipy. X-ray quality crystals were obtained from the slow diffusion of *n*-pentane into a concentrated C_6D_6 solution placed at room temperature in the glovebox. A total of 36 271 reflections ($-15 \le h \le 15$, $-23 \le k \le 23$, $-26 \le l \le 26$) were collected at T = 125(2) K with $2\theta_{max}$ = 56.59°, of which 19 461 were unique (R_{int} = 0.0528). The residual peak and hole electron density were 3.16 and −1.29 e Å^{-3}. There are two independent molecules in the unit cell. Several *tert*-butyl groups were disordered. To some extent, this disorder was modeled with occupancies over two sites. The high residual electron density is due to a small amount of disorder of Si3. This disorder was not modeled. The least-squares refinement converged normally with residuals of R_1 = 0.0772 and GOF = 1.040. A molecule of *n*-pentane was found in the unit cell. Crystal and refinement data for **3-im-bipy**: formula $C_{77}H_{113}N_8Si_4Fe_2Sc_2$, space group $P\bar{1}$, a = 11.7625(14) Å, b = 17.923(2) Å, c = 19.918(2) Å, α = 78.960(1)°, β = 80.862(1)°, γ = 81.288(1)°, V = 4037.3(8) Å^3, Z = 2, μ = 0.621 mm^{-1}, $F(000)$ = 1618, R_1 = 0.1436 and wR_2 = 0.2251 (based on all 19 461 data, $I > 2\sigma(I)$).

DFT Calculations. The Amsterdam Density Functional (ADF) package (version ADF2008.01) was used to do geometry optimizations on Cartesian coordinates of the model compounds specified in the text. For the scandium, yttrium, silicon, and iron atoms, standard triple-ζ STA basis sets from the ADF database ZORA TZP were employed with 1s-2p (Si), 1s-3p (Fe), 1s-3p (Sc), and 1s-4p (Y) electrons treated as frozen cores. For all the other elements, standard double-ζ STA basis sets from the ADF database ZORA DZP were used, with the 1s electrons treated as a frozen core for non-hydrogen atoms. The local density approximation (LDA) by Becke−Perdew was used together with the exchange and correlation corrections that are employed by default by the ADF2008.01 program suite.

Acknowledgment. This work was supported by the UCLA, Sloan Foundation, and NSF (Grant CHE-0847735).

Supporting Information Available: Experimental details for compound characterizations, structural representations indicating a full atom-labeling scheme, DFT calculation details, and full crystallographic descriptions (as cif) are available free of charge via the Internet at http://pubs.acs.org. CCDC numbers for **2-lut**, **3-py^{Ph}-phan**, **3-acr-phan**, **4-py^{Ph}-bqn**, **5-lut-iqn^{Me}**, **6-py^{Et}-iqn^{Me}**, **[2-im]$_2$**, and **3-im-bipy** are 756852, 756853, 756854, 756855, 756856, 756857, 756858, and 756859, respectively.